





RESEARCH ARTICLE

OPEN ACCESS

Chemical composition and cholinesterase, tyrosinase, alpha-amylase and alpha-glucosidase inhibitory activity of the essential oil of *Salvia tomentosa*

Mustafa Kocer^a , Erman Salih Istifli^{b,*} 

^a Kilis 7 Aralik University, Faculty of Science and Literature, Department of Molecular Biology and Genetics, TR-79000, Kilis-Turkey

^b Cukurova University, Faculty of Science and Literature, Department of Biology, TR-01330, Adana-Turkey

ARTICLE INFO

Article History:

Received: 10 October 2021
Revised: 25 October 2021
Accepted: 25 October 2021
Available online: 27 October 2021

Edited by: B. Tepe

Keywords:

Salvia tomentosa
Essential oil
Enzyme inhibitory activity
Molecular docking
ADMET
Drug likeness

ABSTRACT

The aim of this study was to determine the chemical composition of *Salvia tomentosa* (Miller) essential oil and to examine its inhibitory effect on acetylcholinesterase (AChE), butyrylcholinesterase (BChE), tyrosinase, α -amylase and α -glucosidase *in vitro*. In this study, the interaction between the main components of essential oil and the enzymes in question was analyzed through molecular docking analyses. The presence of 60 compounds representing 98.2% of the essential oil was determined. The major compounds of the oil were camphor (9.35%), γ -muurolene (8.37%), α -pinene (7.59%), α -caryophyllene (6.25%), viridiflorol (5.13), δ -cadinene (5.01%), and terpinene-4-ol (5.01 %). The oil exhibited higher inhibitory activity on BChE than on AChE. The BChE inhibitory activity of the oil was determined to be 16.48 mg GALAEs/g. The oil showed 47.13 mg KAEs/g inhibitory activity on tyrosinase. The inhibitory activities of the essential oil on α -glucosidase and α -amylase were determined as 703.29 and 694.75 mg ACEs/g, respectively. Based on docking binding energies, δ -cadinene, viridiflorol, γ -muurolene and α -caryophyllene were determined to be the most promising ligands showing the highest affinity (min. -6.90 kcal/mol; max. -8.40 kcal/mol) against α -amylase, AChE and BChE. However, all four ligands were found to exhibit low affinity (min. -5.50 kcal/mol; max. -5.90 kcal/mol) against tyrosinase. Considering *in silico* physicochemical properties, drug-like features (Lipinski's rule of 5) and intracellular targets, δ -cadinene, viridiflorol, γ -muurolene and α -caryophyllene possess hit features and do not show non-specific enzyme or protein affinity. Ligand binding assays (LBA) to be performed between the monoterpenes and enzymes in question may constitute the next step in confirming their competitive inhibitory capacity.

© 2022 IJPBP. Published by Kilis 7 Aralik University (No: 029). All rights reserved.

1. Introduction

Studies on the use of cholinesterase inhibitors in the treatment of neurodegenerative diseases that cause weakening in cognitive functions such as Alzheimer's disease have been going on for decades. Galanthamine and physostigmine, which are acetylcholinesterase (AChE) inhibitors, can be used temporarily to alleviate the symptoms of the disease. However, these compounds are not suitable for long-term use due to their undesirable side effects. In addition to the compounds mentioned above, many com-

pounds of plant origin can exhibit AChE inhibitory effects. Unfortunately, the effects of these phytochemicals are either not selective or remain limited (Perry and Howes, 2011). Phytochemicals can act on both AChE and butyrylcholinesterase (BChE). However, in the treatment of Alzheimer's disease, the focus is on the discovery of compounds with AChE inhibitory effects. In addition, it is suggested that BChE inhibitors may cause significant regression on the symptoms of the disease and reduce cognitive dysfunction (Li et al., 2008). Many studies have reported that cholinesterases can be inhibited by phytochemicals (Orhan et al., 2018; Orhan et al., 2017; Pinho et al., 2013; Politeo et al., 2018).

Products that reduce hyperpigmentation on the skin have become very popular in recent years, especially in the Asian markets (Pérez Gutierrez et al., 2006). For this reason, researchers began to carry out extensive research on compounds that are effective in

* Corresponding author:

E-mail address: ermansalih@gmail.com (E.S. Istifli)

e-ISSN: 2791-7509

doi:

© 2022 IJPBP. Published by Kilis 7 Aralik University (No: 029). All rights reserved.

lightening dark skin color due to excessive melanin accumulation (Ko et al., 2014; Murata et al., 2014; Tsai et al., 2013). The most critical enzyme involved in the skin pigmentation process is tyrosinase (Fukai et al., 2005). Researchers suggest that compounds with tyrosinase inhibitory effects can overcome skin darkening due to excessive melanin production. Today, there are some compounds with proven tyrosinase inhibitory effects such as hydroquinone, azelaic acid, kojic acid, and arbutin (Chang, 2009; Davis and Callender, 2010). However, it is known that these tyrosinase inhibitors exhibit some side effects such as mutagenicity, irritant and cytotoxicity on the body, and may even cause contact dermatitis or erythema (Lien et al., 2014). Therefore, experts agree that plant-derived compounds can be a natural tyrosinase inhibitory alternative. A large number of tyrosinase inhibitory-effective phytochemicals have been brought to the literature with studies carried out so far (Burlando et al., 2017; Chang, 2012).

Diabetes is an important health problem that affects the metabolism of organic macromolecules, especially carbohydrates, and causes deterioration in many other body functions (Mechchate et al., 2021b; Sacks, 1997). It is estimated that by 2030, the number of diabetic patients will approach 400 million worldwide (Wild et al., 2004). In these patients, some synthetic agents such as α -amylase/ α -glucosidase inhibitors, biguanides and sulfonylureas are used to lower high blood sugar. However, long-term use of these drugs leads to various side effects such as hypoglycemia, nausea, dizziness, and excessive weight gain (Chaudhury et al., 2017; Edwin et al., 2006). Therefore, researchers sought to find safer alternatives to lower blood glucose levels (Es-Safi et al., 2021). Because plants have been used by local people in the treatment of diabetes since ancient times, plants are among the first resources that researchers refer to in search of anti-diabetic compounds (Mechchate et al., 2020; Mechchate et al., 2021a).

Salvia tomentosa (Miller) is one of the most consumed herbal teas. In addition, it has a wound-healing effect similar to iodine tincture. It contains significant amounts of secondary metabolites such as phenolics and terpenoids, which have antimicrobial (Askun et al., 2010; Haznedaroglu et al., 2001) and antioxidant (Erdogan-Orhan et al., 2010) effects. There are some studies on the chemical composition, antimicrobial and insecticidal activity of the essential oil obtained from this plant (Haznedaroglu et al., 2001; Tepe et al., 2005; Ulukanli et al., 2013). In this study, it was aimed to determine the chemical composition of the essential oil obtained from *S. tomentosa*, and to investigate its inhibitory activity on AChE, BChE, tyrosinase, α -amylase and α -glucosidase. In this study, the interaction between phytochemicals and enzymes, which are found in high amounts in the oil, was also examined through molecular docking and it was determined whether these compounds were responsible for the inhibitory activity.

2. Materials and methods

2.1. Plant material

The plant material (*S. tomentosa*) was collected from Osmaniye, Düziçi, Söğütlügöl village. After the plant material was dried in a cool environment without direct sunlight, it was subjected to water distillation for 3 hours using the Clevenger apparatus. Anhydrous sodium sulfate was added to the obtained essential oil to purify it from water, and it was kept at refrigerator temperature (+4 °C) until activity studies were carried out.

2.2. Determination of chemical composition of essential oil

The chemical composition of the essential oil was determined chromatographically by using GC-FID and GC-MS analysis. The analyzes of the oil were performed following the analytical conditions specified in the literature (Sarikurkcu et al., 2015).

2.3. Determination of cholinesterase inhibitory activity

Cholinesterase inhibitory activity test was performed in 96-well microplates using the Ellman method (Ellman et al., 1961). 125 μ l of DTNB, 25 μ l of ATCI or BTCl solutions were added to the microplate wells containing 50 μ l of sample solution. Then, 25 μ l of AChE or BChE solution prepared in tris-HCl buffer (pH 8.0) was added to this mixture. For each sample, a blank sample was prepared using tris-HCl buffer instead of the enzyme solution. All samples were incubated at 25 °C for 15 min and absorbance measurements of both blank and samples were made at 405 nm. The absorbance of the blank sample was subtracted from that of the sample, and the cholinesterase inhibitory activity was expressed as both inhibition (%) and galanthamine equivalents (μ g GALAEs/g sample) (Ellman et al., 1961). Each measurement was made in triplicate and expressed as mean and standard deviation. Galanthamine was used as a positive control.

2.4. Determination of tyrosinase inhibitory activity

The tyrosinase inhibitory activity test was performed in 96-well microplates following the dopachrome method using L-DOPA (40 μ l, 10 mM) as a substrate (Orhan et al., 2014). 100 μ l of phosphate buffer (pH 6.8) and 40 μ l of tyrosinase solution prepared in this buffer were added to the microplate wells containing 25 μ l of sample solution. For each sample, a blank was prepared using phosphate buffer instead of enzyme solution. All samples were incubated for 15 min at 25 °C and absorbance measurements of both blank and sample were performed at 492 nm. The absorbance of the blank was subtracted from that of the sample and the tyrosinase inhibitory activity was calculated in terms of both inhibition (%) and kojic acid equivalent (mg KAEs/g sample) (Orhan et al., 2014). Each measurement was made in triplicate and expressed as mean and standard deviation. Kojic acid was used as a positive control.

2.5. Determination of α -amylase inhibitory activity

The α -amylase inhibitory activity test was performed in 96-well microplates using the Caraway-Somogyi I₂/KI method (Zengin et al., 2014). 50 μ l of starch solution and 25 μ l of α -amylase solution prepared in phosphate buffer (pH 6.9) were added to the microplate wells containing 25 μ l of sample solution. A blank sample was prepared for each sample, using phosphate buffer instead of enzyme solution. All samples were incubated at 25 °C for 15 min and then 25 μ l of HCl solution (1 M) was added to stop the reaction. Then, 100 μ l of I₂/KI was added to all samples and absorbance measurements were performed at 630 nm. The absorbance of the blank was subtracted from that of the sample and the α -amylase inhibitory activity was expressed in terms of both inhibition (%) and acarbose equivalents (mg ACEs/g sample). Each measurement was made in triplicate and expressed as mean and standard deviation. Acarbose was used as a positive control.

2.6. Determination of α -glucosidase inhibitory activity

The inhibitory activity of the essential oil on *S. tomentosa* was determined using the method of Palanisamy et al. (2011). 50 μ l of

PNPG, 50 μ L of glutathione, and 50 μ L of α -glucosidase in phosphate buffer (pH 6.8) were mixed in a 96-well microplate and 50 μ L of sample solution was added onto this mixture. The mixture was incubated for 15 min at 37 $^{\circ}$ C. To prepare the blank, the same mixture without α -glucosidase solution was prepared. The reaction was terminated by adding 50 μ L of 0.2 M sodium carbonate. The absorbance measurements were performed at 400 nm. The absorbance of the blank was subtracted from that of the sample and the α -glucosidase inhibitory activity was expressed as inhibition (%) and acarbose equivalents (mg ACEs/g sample).

2.7. Molecular docking analysis

To reveal the molecular scale contribution of the main essential oil components to the biological activity, *in silico* studies were performed following the method documented by Istifli et al. (2020). In this study, AMDock Vina program was used as the software for docking simulations. AMDock Vina is a graphical tool that facilitates user-friendly docking simulations that can be performed with Autodock Vina or AutoDock4. AMDock Vina uses various external programs (Open Babel, PDB2PQR, AutoLigand, ADT scripts) to prepare input structure files correctly and define an optimal search space. AMDock Vina also provides the option to use Autodock4Zn force field in molecular docking experiments with metalloproteins. Compatible with Windows or Linux, AMDock Vina can be downloaded from <https://github.com/Valdes-Tresanco-MS>. In addition, the UCSF Chimera 1.14 program used for addition of missing atoms in the protein side chains and assigning electrical charges before docking was downloaded from the web address <https://www.cgl.ucsf.edu/chimera/download.html>.

2.7.1. Protein and ligand preparation

In this study, the receptor 3D structures used in molecular docking simulations (human pancreatic α -amylase, human butyrylcholinesterase, human recombinant acetylcholinesterase and Bacillus megaterium tyrosinase) were retrieved from Protein Data Bank (PDB) with codes 1B2Y (resolution: 3.20 \AA), 4BDS (resolution: 2.10 \AA), 4EY6 (resolution: 2.40 \AA) and 5I38 (resolution: 2.60 \AA).

Before docking, inhibitors and heteroatoms (ex. water molecules) complexed with receptors were removed from the crystallographic structures using the Discovery Studio Visualizer v16 program. Calcium and chloride ions in the active site of the α -amylase enzyme and two copper ions in the active site of the tyrosinase enzyme were retained in complex with the catalytic site, since calcium and copper ions are important for these enzymes to perform their physiological functions (Aghajari et al., 2002; Solano, 2018). In general, metal binding affects the stability and catalytic properties of proteins. In addition, the missing atoms and electrical charges in the amino acid side chains of each protein were added using the UCSF Chimera 1.14 program (Pettersen et al., 2004). In our study, the crystallographic structures of α -pinene, camphor, terpinen-4-ol, α -caryophyllene, γ -muurolene, δ -cadinene and viridiflorol were obtained from the PubChem database (<https://pubchem.ncbi.nlm.nih.gov/>) in sdf (structure data file) format and saved in pdb format after performing geometric optimization in the Avogadro program using the MMFF94 (Merck molecular force field) force field suitable for organic molecules (Hanwell et al., 2012).

2.7.2. Molecular docking study

Molecular docking is a bioinformatics method that allows the estimation of the optimal spatial orientation of ligand atoms in the

catalytic cavity of a protein when two biomolecules (protein-ligand or protein-protein) react to form a stable complex under the laws of thermodynamics. In our study, molecular docking calculations of α -pinene, camphor, terpinen-4-ol, α -caryophyllene (α -humulene), γ -muurolene, δ -cadinene and viridiflorol against pancreatic α -amylase, acetylcholinesterase (AChE), butyrylcholinesterase (BChE) and tyrosinase enzymes were carried out. Thus, the lowest energy (most favorable) conformations (pose) of the relevant small molecules in the catalytic sites of these enzymes were predicted and their binding free energies (kcal/mol) were calculated.

AMDock, a docking interface built on the AutoDock Vina algorithm, was implemented for molecular docking calculations of α -pinene, camphor, terpinen-4-ol, α -caryophyllene, γ -muurolene, δ -cadinene and viridiflorol against four enzymes (<https://github.com/Valdes-Tresanco-MS/AMDOck-win>) (Trott and Olson, 2010; Valdes-Tresanco et al., 2020). Grid coordinates (search space) were adjusted to allow ligands to easily interact with the catalytic amino acid residues of these target proteins. In the Discovery Studio Visualizer v16 program, the active sites (groove or pocket) of the four different enzymes were determined by visual inspection of their amino acid residues with which the co-crystallized inhibitors interacted and the corresponding cartesian coordinates were recorded.

Such an approach for the determination of the catalytic site should be logical since it is based on the localization of the experimental inhibitor(s) on the protein molecule. Because the ligand with a similar or more negative binding free energy (binding affinity) compared to the inhibitor may inhibit the protein in question. On the basis of this approach, the grid coordinates (active site) of the target enzymes were adjusted as follows: a) $40 \times 40 \times 40 \text{ \AA}$ (x: 18.90, y: 5.79, z: 47) for the α -amylase; b) $82 \times 56 \times 54 \text{ \AA}$ (x: -9.94, y: -43.48, z: 30.29) for the AChE; c) $70 \times 62 \times 54 \text{ \AA}$ (x: 132.99, y: -116.01, z: 41.21) for the BChE and, d) $48 \times 50 \times 52 \text{ \AA}$ (x: 1.85, y: 101.73, z: 25.19) for the tyrosinase.

In the configuration settings prepared for molecular docking, the value of 'exhaustiveness' was set as '56' and the number of independent docking runs (number of poses) was set as '20'. In each docking iteration, all potential binding modes (conformations) of α -pinene, camphor, terpinen-4-ol, α -caryophyllene, γ -muurolene, δ -cadinene, and viridiflorol were clustered by AutoDock Vina, and the ligand conformations obtained against α -amylase, AChE, BChE and tyrosinase enzymes were ranked from the most negative to the least according to their binding free energies (ΔG° ; kcal/mol). The best docking poses calculated by AMDock against protein targets of the seven ligands studied were visualized using the Discovery Studio Visualizer v16 program, and non-covalent chemical interactions were characterized at the molecular level.

2.8. Determination of 'relative binding capacity index' (RBCI) values of essential oil major components

RBCI values were calculated considering the affinities of the main components in the essential oil for all targets. For this purpose, the method developed by Istifli et al. (2020) was followed. Thus, 'hit' components showing higher affinity for all target structures were identified and the best poses (top-ranked conformations) of these components were presented.

2.9. Clarification of ADMET and drug-likeness profiles of 'hit' compounds, identification of possible intracellular targets

Identification of drug-likeness, absorption-distribution-metabolism-excretion and toxicity (ADMET) and intracellular target profiles of

promising 'hit' compounds in structure-based drug design (SBDD) studies is crucial to understand possible side effects of these bioactive molecules on the target organism. In this study, web-based SwissADME, pkCSM and SwissTargetPrediction tools were used to analyze such effects of the terpenoids in question (Daina et al., 2017; Daina et al., 2019; Delaney, 2004; Pires et al., 2015). In addition, the interaction probabilities of 'hit' molecules with various classes of intracellular targets were also given as maximum and minimum numerical values. ADMET and drug-likeness profiles and possible intracellular targets of the compounds identified as 'hit' as a result of RBCI analyzes were determined according to Istifli et al (2020).

3. Results and discussion

3.1. Chemical composition of the essential oil

The chemical composition of the essential oil was determined chromatographically by GC-FID and GC-MS analysis. The data obtained are given in Table 1.

According to the data in Table 1, the presence of 60 compounds representing 98.2% of the essential oil was determined as a result of the quantitative chromatographic analyzes performed. The major compounds of the oil were camphor (9.35%), γ -muurolene (8.37%), α -pinene (7.59%), α -caryophyllene (6.25%), viridiflorol (5.13), δ -cadinene (5.01%), and terpinene-4-ol (5.01 %).

As a result of the literature research, some studies were found in which the chemical composition of *S. tomentosa* essential oil was investigated (Askun et al., 2010; Bardakci et al., 2019; Hanlidou et al., 2014; Haznedaroglu et al., 2001; Nagy et al., 1999; Özcan et al., 2002; Soltanbeigi and Sakartepe, 2020; Tepe et al., 2005; Ulubelen et al., 1981a, b; Ulukanli et al., 2013; Yilar et al., 2018). In these studies, the presence of α -pinene, β -pinene, 1,8-cineole, borneol, camphor, α -thujene, *cis*-thujone, camphene, α -caryophyllene, cyclofenchene, δ -cadinene, some diterpenoids and triterpenoids were reported as main components.

The essential oil data obtained from the present study are largely in agreement with the literature data. However, some of the major compounds (terpinene-4-ol, α -caryophyllene, γ -muurolene and viridiflorol) determined in the current study were not found as major compounds in previous studies with the essential oil of the plant in question. This difference is thought to be caused by factors such as differences in the area where the plant is collected, climate and soil structure, harvest time, etc.

3.2. Cholinesterase inhibitory activity potential of the essential oil

The data obtained from the AChE and BChE inhibitory activity tests of *S. tomentosa* essential oil are given in Table 2. The data in the table in question were presented in terms of both positive control (galanthamine) equivalent and IC₅₀ (mg/ml).

The essential oil exhibited higher inhibitory activity on BChE than on AChE in terms of galanthamine equivalent. This situation is also reflected in the enzyme inhibitor activity data calculated in terms of IC₅₀. The BChE inhibitory activity of the essential oil was determined to be 16.48 mg GALAEs/g essential oil and 1.30 mg/ml in terms of galanthamine equivalent and IC₅₀, respectively. As can be seen from the data in the table, the essential oil exhibited quite low activity compared to galanthamine.

Table 1. Chemical composition of the essential oil of *S. tomentosa*

No	KI	Compound	Amount (%)
1	926	α -Thujene	0.16
2	935	α -Pinene	7.59
3	947	Camphene	1.66
4	974	β -Pinene	4.16
5	990	β -Myrcene	1.04
6	999	α -Phellandrene	0.40
7	1010	α -Terpinene	1.57
8	1028	Limonene	3.93
9	1035	<i>cis</i> -Ocimene	3.72
10	1050	γ -Terpinene	3.36
11	1061	<i>cis</i> -Sabinene hydrate	0.78
12	1065	<i>cis</i> -Linalool oxide (furanoid)	1.59
13	1074	<i>p</i> -cymenene	0.23
14	1079	Terpinolene	0.59
15	1083	Nonanal	0.13
16	1085	α -Pinene oxide	0.87
17	1097	<i>trans</i> -Sabinene hydrate	0.43
18	1099	Linalool	0.89
19	1105	<i>cis</i> -Thujone	0.43
20	1115	<i>trans</i> -Thujone	1.15
21	1125	α -Campholenal	0.68
22	1136	<i>trans</i> -Pinocarveol	1.24
23	1143	Camphor	9.35
24	1154	Borneol	4.05
25	1158	<i>cis</i> -Pinocampnone	0.21
26	1176	Terpinen-4-ol	5.01
27	1186	α -Terpineol	0.66
28	1286	Bornyl acetate	3.89
29	1330	α -Terpinyl acetate	0.21
30	1350	α -Cubebene	0.26
31	1370	α -Ylangene	0.29
32	1374	α -Copaene	0.18
33	1382	β -Bourbonene	0.37
34	1385	β -Cubebene	0.19
35	1439	Aromadendrene	0.23
36	1455	α -Caryophyllene	6.25
37	1477	γ -Muurolene	8.37
38	1481	α -Amorphene	0.94
39	1485	Germacrene D	1.27
40	1514	δ -Cadinene	0.72
41	1523	δ -Cadinene	5.01
42	1527	α -Cadinene	0.77
43	1532	α -Calacorene	0.30
44	1535	Germacrene B	0.19
45	1537	β -Elemol	0.36
46	1538	Selina-3.7(11)-diene	0.25
47	1547	β -Calacorene	1.14
48	1550	(<i>E</i>)-Nerolidol	0.13
49	1562	Palustrol	0.68
50	1568	Germacrene-D-4-ol	0.26
51	1571	Ledol	0.71
52	1575	(-)-Spathulenol	0.85
53	1593	Viridiflorol	5.13
54	1602	Guaiol	0.55
55	1639	τ -Cadinol	0.54
56	1646	α -Cadinol	0.50
57	1648	α -Muurolol	0.47
58	1670	Cadalene	0.56
59	1672	<i>epi</i> - β -Bisabolol	0.36
60	1687	α -Bisabolol	0.39
		Total	98.2

There is no study in the literature on the cholinesterase inhibitory activity of *S. tomentosa* essential oil. However, it is possible to refer to some literature data on the contribution of the oil major compounds to cholinesterase inhibitory activity. In a study investigating the inhibitory effect of camphor and α -pinene on human erythrocyte AChE, the inhibitory activity of α -pinene was found to be 0.63 mM, while camphor provided non-competitive reversible inhibition on the enzyme in question (Perry et al., 2000). This data reported for camphor has been confirmed by other researchers (Lopez et al., 2015; Savelev et al., 2003). In a study conducted by Ertas et al. (2014), it was determined that the essential oil obtained from *Lycopsis orientalis* contained 9.6% *tau*-muurolene (γ -muurolene isomer) as the major compound and

showed significant inhibitory activity on both AChE and BChE at a concentration of 200 µg/ml. In another study investigating the inhibitory activities of caryophyllene and terpinen-4-ol, the inhibitory activities of these terpenoids against BChE were determined to be 78.6 and 107.6 µg/ml in terms of IC₅₀, respectively

(Bonesi et al., 2010). In the literature, no study was found that δ-cadinene and viridiflorol can contribute to cholinesterase inhibitory activity.

Table 2. Enzyme inhibitory activity potential of *S. tomentosa* essential oil

Enzyme	EC number	CAS number	Positive control equivalent activity	IC ₅₀ (mg/ml)	Galanthamine	Kojic acid	Acarbose
AChE ¹	3.1.1.7	9000-81-1	3.26 ± 0.47	1.35 ± 0.19	0.0043 ± 0.0003	-	-
BChE ¹	3.1.1.8	9001-08-5	16.48 ± 0.39	1.30 ± 0.03	0.0022 ± 0.0006 ^a	-	-
Tyrosinase ²	1.14.18.1	9002-10-2	47.13 ± 0.95	1.73 ± 0.03	-	0.08 ± 0.002	-
α-Amylase ³	3.2.1.1	9000-90-2	694.75 ± 10.78	1.51 ± 0.02	-	-	1.05 ± 0.04
α-Glucosidase ³	3.2.1.10	9001-42-7	703.29 ± 8.02	0.97 ± 0.01	-	-	0.68 ± 0.04

¹ mg GALAEs/g essential oil, ² mg KAEs/g essential oil, ³ mg ACEs/g essential oil

3.3. Tyrosinase inhibitory activity potential of the essential oil

The data obtained from the tyrosinase inhibitory activity test of *S. tomentosa* essential oil are given in Table 2. The data in the table in question are presented in terms of both positive control (kojic acid) equivalents and IC₅₀ (mg/ml).

As can be seen from Table 2, the essential oil of *S. tomentosa* showed 47.13 mg KAEs/g activity on tyrosinase in terms of kojic acid equivalent. The equivalent of this activity in terms of IC₅₀ was determined as 1.73 mg/ml. In the same test system, kojic acid itself exhibited inhibitory activity on tyrosinase with an IC₅₀ value of 0.08 mg/ml.

There are no reports in the literature regarding the tyrosinase inhibitory activity of *S. tomentosa* essential oil. However, there are some reports of tyrosinase inhibitory activities of essential oil major compounds themselves or essential oil samples containing these components in high amounts. In a study conducted by Ho (2010), *Alpinia speciosa* seed oil containing camphor, terpinen-4-ol and α-pinene as major compounds showed an inhibitory effect between 74-81% at 1000 ppm concentration on fungal tyrosinase. In another study conducted by Haliloglu (2017), it was stated that the essential oil of *Achillea sivasica* contained α-pinene and camphor as major compounds and showed significant anti-tyrosinase activity. There are also studies in the literature that caryophyllene inhibits melanogenesis, thus tyrosinase activity. In a study by Yang et al. (2015), it was reported that the aforementioned terpenoid inhibits melanogenesis by inhibiting MITF, TRP-1, TRP-2 and tyrosinase. There are also reports in the literature that various essential oils, including γ-murolene, δ-cadinene, and viridiflorol as major compounds, show remarkable tyrosinase inhibitory activities (Elgamal et al., 2021; Salleh et al., 2015).

3.4. α-Amylase and α-glucosidase inhibitory activity potential of the essential oil

The data obtained from the α-amylase and α-glucosidase inhibitory activity tests of *S. tomentosa* essential oil are given in Table 2. The data in the table in question are presented in terms of both positive control (acarbose) equivalents and IC₅₀ (mg/ml).

Although the inhibitory activity values on the enzymes were quite close to each other, according to the data in the table, *S. tomentosa* essential oil exhibited a slightly higher inhibitory activity on α-glucosidase than on α-amylase. However, in the calculations made in terms of IC₅₀, the α-glucosidase inhibitory activity of the oil was found to be approximately 30% higher than the α-amylase inhibitory activity. The inhibitory activities of the essential oil on α-glucosidase and α-amylase were determined as 703.29 and 694.75 mg ACEs/g

essential oil in terms of acarbose equivalent, respectively. Acarbose, used as a positive control in the same test system, showed stronger activity on these enzymes than the essential oil. However, the α-amylase inhibitory activity of the oil was found to be significant, comparable to acarbose.

As a result of the literature search, no report was found that investigated the inhibitory effect of the extract and/or essential oil obtained from *S. tomentosa* on digestive enzymes. However, there are some reports that the major compounds of essential oil may contribute to the inhibitory activity on these enzymes. In a study by Ferrante et al. (2019), it was reported that *Artemisia santonicum* essential oil containing 36.6% camphor exhibited significant inhibitory activity on both digestive enzymes. Findings put forward by Jugreet et al. (2020) also support these data. In another study, *Hertia cheirifolia* essential oil, which contains high amounts of α-pinene as the major compound, was stated to be a potential α-glucosidase inhibitor (Majouli et al., 2016). In a molecular docking study conducted by Yang et al. (2019), it was stated that the binding score of α-pinene to α-amylase was high, while in the same study, it was stated that the binding scores were low for caryophyllene and cadinene. Although there are some reports in the literature that some plant species containing terpinen-4-ol as the main component exhibit remarkable α-amylase and α-glucosidase inhibitory activities (Bouyahya et al., 2020; Usman et al., 2020) viridiflorol is not mentioned. No report has been found regarding its effectiveness on the enzymes in question.

3.5. Molecular docking results of essential oil major compounds

Molecular docking is a widely used method in structure-based drug design (SBDD) due to its ability to predict the binding conformation of small molecules on respective target proteins with a high degree of precision (Ballante, 2018; Dos Santos et al., 2018; Meng et al., 2011; Wang et al., 2020). Molecular docking programs, the first known algorithms of which were written in 1980s, have now become an essential tool in drug discovery (Lohning et al., 2017; Lopez-Vallejo et al., 2011). Using this method, important intermolecular biochemical reactions such as the binding conformations of ligands to their respective receptors and interactions that stabilize the ligand-receptor system can be easily analyzed and visualized (Huang and Zou, 2010). In addition, molecular docking algorithms perform quantitative estimations of receptor-ligand binding energies, enabling the 'docked' conformations of the simulated ligands to be ranked, taking into account their binding free energies (Ferreira et al., 2015; Huang and Zou, 2010; Lopez-Vallejo et al., 2011).

In this study, molecular interactions between target proteins (α-amylase, AChE, BChE, and tyrosinase) and 7 terpenoids (δ-cadinene, viridiflorol, γ-murolene, α-caryophyllene, terpinen-4-ol, camphor,

and α -pinene) were investigated via molecular docking simulations. Subsequently, the binding free energy (binding affinity) of each ligand was predicted, and the stabilizing non-bonded interactions were characterized by visualizing top-ranked ligand-receptor conformations. However, as a result of the RBCI analysis, the interactions of only 4 compounds (δ -cadinene, viridiflorol, γ -

muurolene and α -caryophyllene) determined as 'hit' were given (Tables 4, 5, 6 and 7). The binding free energy (ΔG° , kcal/mol) and inhibition constant (K_i , μM) of these four 'hit' phytochemicals for which molecular docking simulations were performed are given in Table 3.

Table 3. Binding free energy and inhibition constant of 'hit' terpenoids determined in molecular docking

Molecule	Binding free energy (kcal/mol)				Inhibition constant (μM)			
	α -Amylase	AChE	BChE	Tyrosinase	α -Amylase	AChE	BChE	Tyrosinase
δ -Cadinene	-7.10	-8.40	-7.50	-5.90	6.25	0.69	3.18	47.35
Viridiflorol	-7.50	-7.80	-7.70	-5.70	3.18	1.92	2.27	66.36
γ -Muurolene	-6.90	-8.00	-7.50	-5.80	8.76	1.37	3.18	56.05
α -Caryophyllene	-7.40	-8.30	-7.10	-5.50	3.77	1.37	6.25	93

The top-ranked conformation of δ -cadinene in the binding cavity of the human pancreatic α -amylase enzyme and the types of amino acid molecular interactions are given in Figure 1A and Table 4. While δ -cadinene formed alkyl interactions with Leu161 and Leu164 residues of human pancreatic α -amylase enzyme and pi-alkyl interactions with Trp58, Tyr61 and His298 residues, it formed a pi-

sigma interaction with Tyr61 (Table 4). All the chemical bonds induced by δ -cadinene in the catalytic pocket of α -amylase enzyme are hydrophobic type (Table 4). δ -cadinene binds with high affinity to the binding cavity of the pancreatic α -amylase enzyme (-7.10 kcal/mol, Table 3).

Table 4. Amino acid molecular interactions between human pancreatic α -amylase and 'hit' terpenoids and types of formed chemical interactions¹

Molecule	Classical H-bond	Van der Waals	Non-classical H-bond (C-H, PI-Donor)	Hydrophobic		Electrostatic	Miscellaneous (Lone pair/PI-sulphur)
				π - π interaction	Mixed π /Alkyl		
δ -Cadinene	-	-	-	-	Trp58, Tyr61, Leu161, Leu164, His298	-	-
Viridiflorol	-	-	-	-	Trp57, Trp58, Tyr61, Leu161, Leu164, His304	-	-
γ -Muurolene	-	-	-	-	Trp58, Tyr61, Leu161, Leu164, His298	-	-
α -Caryophyllene	-	-	-	-	Trp57, Trp58, Tyr61, Leu164, His304	-	-

¹ Asp197, Glu233 and Asp300 are active site residues that play direct role in the catalytic function of the human pancreatic α -amylase.

The types of amino acid molecular interactions and top-ranked conformation of δ -cadinene in the catalytic pocket of human AChE enzyme are given in Figure 1B and Table 5. As a result of the docking simulation, δ -cadinene formed pi-alkyl interactions with AChE's Trp83, Tyr121, Phe288, Phe329, His438 and Tyr440 residues, and pi-sigma bonds with the Tyr328. The chemical bonds induced by δ -cadinene in the binding cavity of the AChE are all hydrophobic type (Table 5). δ -cadinene binds to the catalytic pocket of the human AChE enzyme with a very favorable affinity (-8.40 kcal/mol, Table 3).

In a molecular simulation study performed by Hussein et al. (2019), it was found that the bicyclic sesquiterpene δ -cadinene, present in the total extract of the *Commiphora myrrha* (Nees) plant, bound to the human AChE with a very high affinity of -9.2 kcal/mol, and formed hydrophobic contacts with Trp83, Phe330 and His439 residues localized in the catalytic triad of the enzyme (Hussein et al., 2019). In another *in silico* study, δ -cadinene exhibited a binding affinity of -6.77 kcal/mol to AChE, the target protein of Alzheimer's disease, and formed pi-alkyl bonds with polar aliphatic residues Trp286 and His447, and hydrophobic contacts with hydrophobic residues Tyr124 and Phe295 (da Silva Barbosa et al., 2020). Although the results of our study show some differences from the above-mentioned two *in silico* studies in terms of the amino acid residues to which δ -cadinene binds, δ -cadinene generally forms hydrophobic contacts with residues bearing cyclic side chains in AChE, and

therefore, our results are in agreement with the other two *in silico* studies in this respect. Furthermore, the wide active site (active gorge) of AChE displays high variability, and the X-ray crystallographic structures obtained to date proved that the aromatic residues (Trp286 and Tyr337) that fall within the P (peripheral)- and A (acylation)-sites of the enzyme demonstrates high mobility in their ligand binding patterns (Rosenberry et al., 2017).

The top-ranked conformation of δ -cadinene in the catalytic cavity of the human BChE enzyme is given in Figure 1C. While δ -cadinene formed pi-alkyl contacts with Trp79, Tyr329, Trp425, His433 and Tyr435 residues of human BChE enzyme, it formed alkyl bonds with Ala325 and Met432 residues as well as some additional pi-sigma bonds with Tyr79 residue (Table 6). Notably, both the Ala325 and Tyr329 residues are located in the active site of the BChE enzyme, and the Tyr329 residue is located in the A (acylation)-site of the active site pocket (Rosenberry et al., 2017). As a result, δ -cadinene entered an energetically favorable (exergonic) binding reaction at the active site of the human BChE enzyme and formed non-bonded interactions preferably with hydrophobic amino acids.

Since the crystal structure of the human tyrosinase enzyme has not been clarified yet, the molecular docking simulations of the tyrosinase enzyme in this study were performed on the tyrosinase

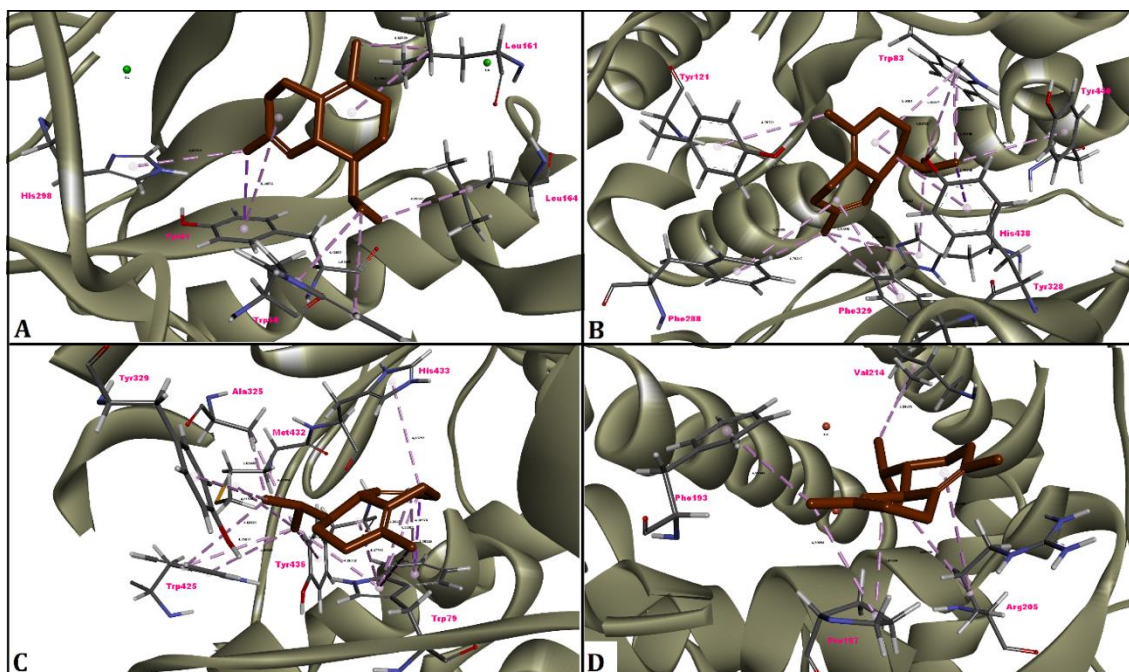


Figure 1. Top-ranked conformations of δ -cadinene (A- α -amylase, B- AChE, C- BChE, D- Tyrosinase)

enzyme (PDB ID: 5I38) isolated from *Bacillus megaterium* (Noh et al., 2020). The top-ranked conformation of δ -cadinene in the active site of the *B. megaterium* tyrosinase enzyme is given in Figure 1D. δ -cadinene formed alkyl contacts with the Pro197, Arg205 and Val214

residues and pi-alkyl bonds with the Phe193 residue of *B. megaterium* tyrosinase (Table 7). In *B. megaterium* tyrosinase, Met61 and Met184 residues play a catalytic role in the transfer of

Table 5. Amino acid molecular interactions between human AChE and 'hit' terpenoids and types of formed chemical interactions¹

Molecule	Classical H-bond	Van der Waals	Non-classical H-bond (C-H, Pi-Donor)	Hydrophobic		Electrostatic	Miscellaneous (Lone pair/Pi-sulphur)
				π - π interaction	Mixed π /Alkyl		
δ -Cadinene	-	-	-	-	Trp83, Tyr121, Phe288, Tyr328, Phe329, His438, Tyr440	-	-
Viridiflorol	-	-	His438	-	Trp83, Tyr121, Phe288, Tyr328, Phe329, His438	-	-
γ -Muurolene	-	-	-	-	Trp83, Tyr121, Phe288, Tyr328, His438, Tyr440	-	-
α -Caryophyllene	-	-	-	-	Trp83, Tyr328, Phe329, His438	-	-

¹ Tyr72, Asp74, Trp86, Tyr121, Tyr124, Tyr133, Glu202, Ser203, Ser229, Trp236, Trp286, Phe295, Phe297, Phe288, Glu334, Tyr337, Phe338, Tyr341, His440 and His447 are directly involved in the catalytic function of the human AChE.

Table 6. Amino acid molecular interactions between human BChE and 'hit' terpenoids and types of formed chemical interactions¹

Molecule	Classical H-bond	Van der Waals	Non-classical H-bond (C-H, Pi-Donor)	Hydrophobic		Electrostatic	Miscellaneous (Lone pair/Pi-sulphur)
				π - π interaction	Mixed π /Alkyl		
δ -Cadinene	-	-	-	-	Trp79, Ala325, Tyr329, Trp425, Met432, His433, Tyr435	-	-
Viridiflorol	-	-	-	-	Trp79, Phe326, His433	-	-
γ -Muurolene	-	-	-	-	Trp79, Ala325, Phe326, Met432, His433, Tyr435	-	-
α -Caryophyllene	-	-	-	-	Trp79, Ala325, Tyr329, Trp425	-	-

¹Active site residues that play a direct role in the catalytic function of human BChE (Asn68, Asp70, Trp82, Gln119, Tyr128, Glu197, Ser198, Ser224, Trp231, Ala277, Leu286, Val288, Glu(Ala)325, Ala328, Phe(Tyr)329, Tyr332, Phe398, His438). The residues given in parentheses (Ala325, Tyr329) are silent mutations that occur as a result of polymorphism in the DNA molecule, however, have no effect on the catalytic function of the enzyme.

copper ions to the flexible His60 residue, thereby positioning copper ions in the active site. *B. megaterium* tyrosinase enzyme (PDB ID:

5I38) used in docking calculations in this study shows some differences in terms of active site residues reported in the literature

(Noh et al., 2020). For instance, histidine at position 60 has changed to alanine, methionine at position 61 to phenylalanine, and

methionine at position 184 to asparagine. It can be envisioned that these substitutions could be due to the polymorphism in bacterial

Table 7. Amino acid molecular interactions and types of chemical interactions between *B. megaterium* tyrosinase and 'hit' terpenoids 1

Molecule	Classical H-bond	Van der Waals	Non-classical H-bond (C-H, Pi-Donor)	Hydrophobic		Electrostatic	Miscellaneous (Lone pair/Pi-sulphur)
				π - π interaction	Mixed π /Alkyl		
δ -Cadinene	-	-	-	-	Phe193, Pro197, Arg205, Val214	-	-
Viridiflorol	Gly209	Gly212	-	-	Phe120, Ala151	-	-
γ -Muuroolene	-	-	-	-	Pro197, His204, Arg205, Val213, Val214, Ala217	-	-
α -Caryophyllene	-	-	-	-	Arg161, Val164, Leu165, Val236, Ile284	-	-

¹ His60, Met61 and Met184 are active site residues that play direct role in the catalytic function of the *B. megaterium* tyrosinase.

DNA at the molecular level, but the altered amino acid sequence is a silent mutation that does not adversely affect the catalytic function of the enzyme. In this study, although δ -cadinene did not form chemical contacts with Ala60, Phe61 and Asn184 residues of the tyrosinase enzyme, the amino acids it interacts with (Phe193, Pro197, Arg205 and Val214) are positionally close to Ala60 and Phe61, however, due to the low binding energy (-5.90 kcal/mol) it

can be said that the possibility of a competitive inhibition is low. Consistent with this study, Ak et al. (2021) reported a low GOLD fitness score (38.92) of δ -cadinene against the tyrosinase enzyme isolated from the fungus (PDB ID: 2Y9X). Taken together, the results from both studies indicate that δ -cadinene is not a favorable competitive inhibitor for the tyrosinase enzyme.

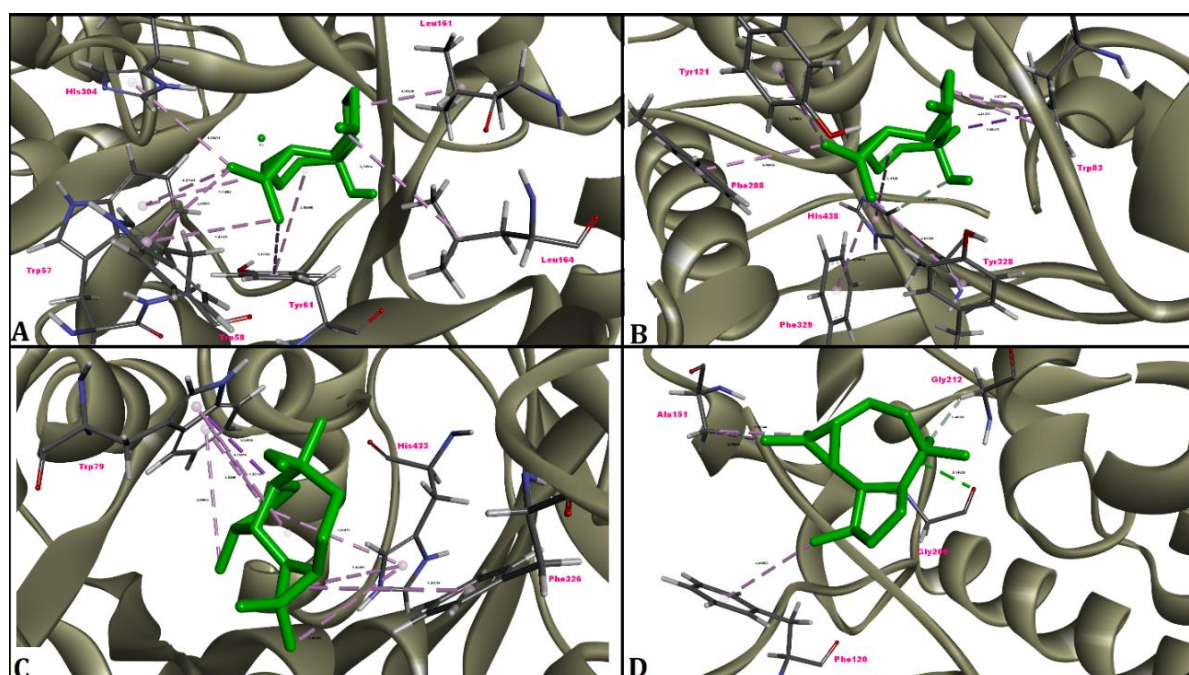


Figure 2. Top-ranked conformations of viridiflorol (A- α -amylase, B- AChE, C- BChE, D- Tyrosinase)

The top-ranked conformation of viridiflorol in the binding pocket of the human pancreatic α -amylase enzyme is shown in Figure 2A. Viridiflorol formed hydrophobic pi-alkyl contacts and alkyl bonds with Leu161 and Leu164 with Trp57, Trp58, Tyr61 and His304 residues of the human pancreatic α -amylase enzyme (Table 4). Viridiflorol exhibited a very favorable binding with the α -amylase enzyme (-7.50 kcal/mol, Table 3) and was localized in the vicinity of the active site residues (Asp197, Glu233, Asp300) reported in the literature (Brayer et al., 1995). The top-ranked conformation of viridiflorol in the inhibitor binding cavity of the human AChE enzyme is given in Figure 2B. Viridiflorol formed pi-alkyl contacts with the Trp83, Tyr121, Phe288, Tyr328, Phe329 and His438 residues of AChE, a pi-sigma bond with Trp83, and a carbon-hydrogen bond with His438 (Table 5). The affinity of the hydrophobic viridiflorol molecule against the active pocket of the human AChE enzyme was

found to be quite favorable (-7.80 kcal/mol, Table 3). The top-ranked conformation of viridiflorol in the inhibitor binding pocket of the human BChE enzyme is given in Figure 2C. Viridiflorol formed pi-alkyl bonds and a pi-sigma bond with the Trp79, Phe326 and His433 residues of BChE (Table 6). Moreover, viridiflorol exhibited an energetically favorable binding (-7.70 kcal/mol) with BChE and displayed a higher binding affinity than AChE (Table 3). The top-ranked conformation of viridiflorol in the active site of the *B. megaterium* tyrosinase is shown in Figure 2D. Viridiflorol formed alkyl and pi-alkyl bonds with Phe120 and Ala151 residues, classical hydrogen bonds with Gly209, and carbon-hydrogen bonds with Gly212 residues of *B. megaterium* tyrosinase (Table 7). The affinity of viridiflorol against the active site of the *B. megaterium* tyrosinase enzyme is energetically less favorable (-5.70 kcal/mol, Table 3). Consistent with these results, Ak et al. (2021) reported that

viridiflorol exhibited a low GOLD fitness score (33.71) against the fungal tyrosinase (PDB ID: 2Y9X). The top-ranked conformation of γ -muurolene in the binding pocket of the human pancreatic α -amylase enzyme is shown in Figure 3A. γ -Muurolene formed pi-alkyl bonds with the Trp58, Tyr61 and His298 residues of the human α -amylase enzyme, alkyl bonds with Leu161 and Leu164, and

additional pi-sigma bonds with Tyr61 (Table 4). The affinity of γ -muurolene against the active site of α -amylase is moderately strong (-6.90 kcal/mol, Table 3). However, this docking binding score of the same ligand is more favorable than the binding energy (-5.59 kcal/mol) determined by Yang et al. (2019) against α -amylase. The

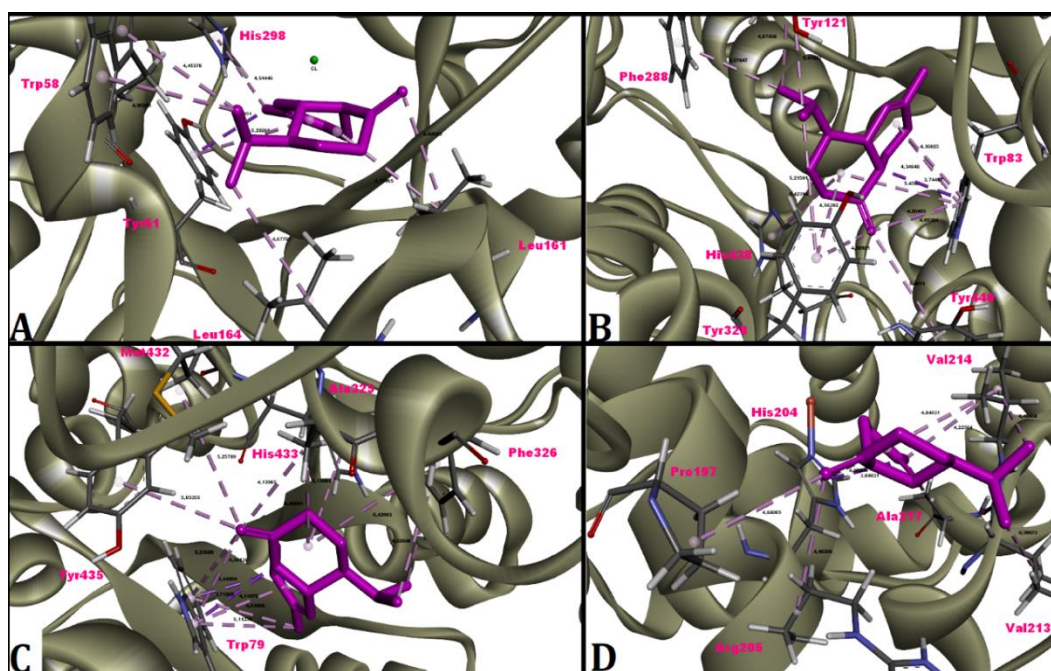


Figure 3. Top-ranked conformations of γ -muurolene (A- α -amylase, B- AChE, C- BChE, D- Tyrosinase)

better binding affinity scored by AutoDock Vina program compared with the score found by Yang et al. (2019) shows that AutoDock Vina has a more optimized scoring function than the AutoDock 4.2, and thus can identify energetically more favorable binding conformations in the active site of the α -amylase. The top-ranked conformation of γ -muurolene in the inhibitor binding cavity of the human AChE enzyme is given in Figure 3B. The interaction of γ -muurolene with the catalytic pocket of AChE is energetically very favorable (-8.00 kcal/mol, Table 3). While γ -muurolene formed pi-alkyl contacts with AChE residues Trp83, Tyr121, Phe288, Tyr328, His438 and Tyr440, it also formed pi-sigma bonds with Trp83 (Table 5). The top-ranked conformation of γ -muurolene in the binding pocket of human BChE enzyme is given in Figure 3C. γ -muurolene formed pi-alkyl bonds with Trp79, Phe326, His433 and Tyr435 residues of the BChE enzyme, pi-sigma bonds with Trp79, as well as alkyl bonds with Ala325 and Met432 (Table 6). The interaction of γ -muurolene with the active site of the BChE enzyme is energetically very favorable (-7.50 kcal/mol, Table 3). The top-ranked conformation of γ -muurolene in the active site of *B. megaterium* tyrosinase enzyme is shown in Figure 3D. γ -Muurolene formed alkyl bonds with Pro197, Arg205, Val213, Val214 and Ala217 residues of *B. megaterium* tyrosinase, and pi-alkyl and pi-sigma bonds with His204 (Table 7). The docking-binding affinity of γ -muurolene for *B. megaterium* tyrosinase is energetically not very favorable (-5.80 kcal/mol, Table 3). Sinan et al. (2021), reported that γ -muurolene exhibited a low GOLD fitness score (40.31) against tyrosinase enzyme, confirming the result of our study, in their chemodiversity and biological activity research.

The top-ranked conformation of α -caryophyllene in the active site of the human pancreatic α -amylase enzyme is given in Figure 4A. Alpha-caryophyllene formed pi-alkyl bonds with the Trp57, Trp58,

Tyr61 and His304 residues in the active site of the enzyme as well as alkyl bonds with Leu164 (Table 4). The interaction of α -caryophyllene with the active site of the pancreatic α -amylase is energetically very favorable (-7.40 kcal/mol, Table 3). The top-ranked conformation of α -caryophyllene in the active site of the human AChE enzyme is given in Figure 4B. α -Caryophyllene formed pi-alkyl contacts with Trp83, Tyr328, Phe329 and His438 residues of the enzyme as well as a pi-sigma contact with Tyr328 (Table 5). The interaction of alpha-caryophyllene with residues in the active site of the AChE enzyme is energetically highly favorable (-8.30 kcal/mol, Table 3). Consistent with our docking results, Karimi et al. (2021) reported that α -caryophyllene in the herbal extract of *Cannabis sativa* L. showed a binding affinity of -9.00 kcal/mol with the AChE and formed hydrophobic contacts with the Asp71, Trp83 and Tyr120.

The top-ranked conformation of α -caryophyllene in the active site of the human BChE enzyme is shown in Figure 4C. Alpha-caryophyllene formed pi-alkyl bonds with Trp79, Tyr329 and Trp425 residues of BChE as well as alkyl bonds with the Ala325 (Table 6). The interaction of α -caryophyllene with the active site of the BChE enzyme is energetically favorable (-7.10 kcal/mol, Table 3). In support of our results, Karimi et al. (2021) found that α -caryophyllene in the herbal extract of *C. sativa* plant showed a favorable binding affinity of -7.70 kcal/mol for BChE active site, and formed hydrophobic interactions with residues His433, Asp67 and Try329 in the peripheral anionic site (PAS), as well as Trp79, Ala325 and Phe326 in the acylation site (AS).

In molecular docking studies, it may be necessary to examine the binding poses of ligands which display favorable binding energetics (high affinity) and to check whether the binding event takes place in

the correct cavity (active site) of the enzyme. Because, although a ligand shows a highly negative binding free energy, the binding

event can sometimes occur in a location outside the active site of the enzyme that has multiple binding sites. Therefore, to examine

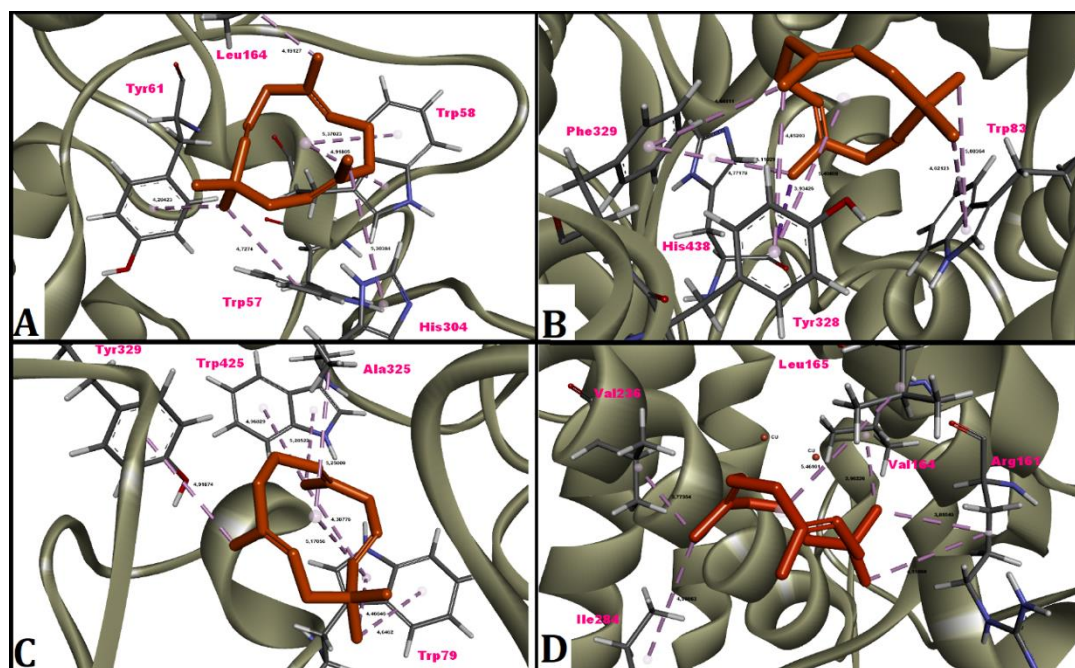


Figure 4. Top-ranked conformations of α -caryophyllene (A- α -amylase, B- AChE, C- BChE, D- Tyrosinase)

this issue, the top-ranked poses of the four 'hit' ligands were superposed on the active site with the binding pose of the co-crystallized inhibitors on the hydrophobicity surfaces of α -amylase, AChE, BChE and tyrosinase (Figures 5-8). Delta-cadinene, viridiflorol, γ -muurolene and α -caryophyllene were all found to be colocalized

with acarbose in the active site of human pancreatic α -amylase enzyme. Thus, the docking scoring function produced a 'true positive' result for the α -amylase enzyme (Figure 5A, B, C, D). Delta-

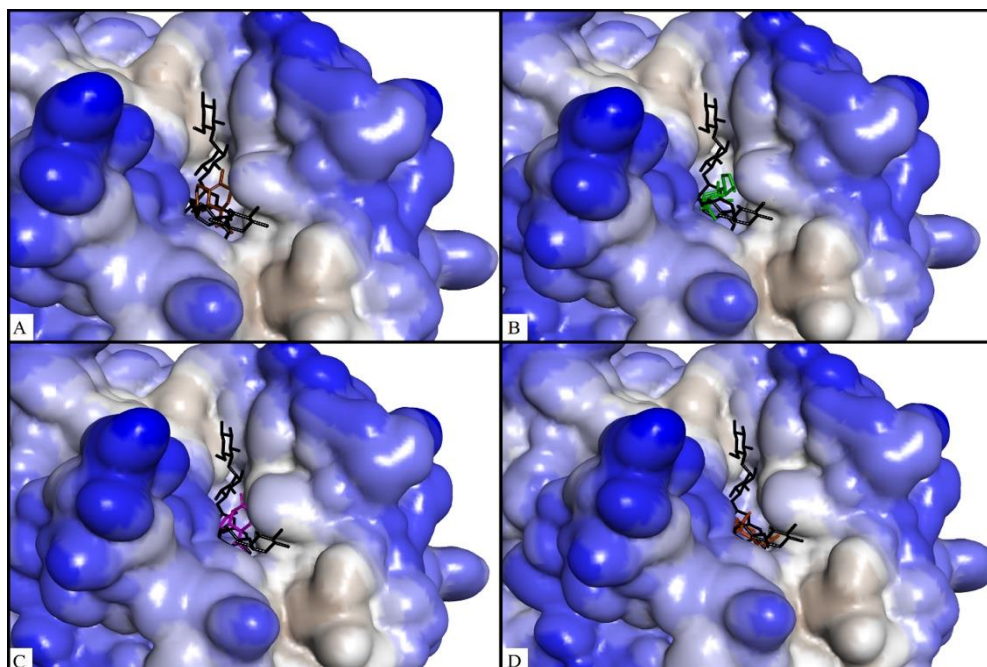


Figure 5. Superposed images of co-crystallized inhibitor (acarbose, black) with δ -cadinene (A), viridiflorol (B), γ -muurolene (C), and α -caryophyllene (D) ligands in the active site of human pancreatic alpha-amylase

cadinene, viridiflorol, γ -muurolene and α -caryophyllene colocalized with galanthamine at the active site of the human AChE enzyme. Thus, the docking scoring function produced a 'true positive' result

for the AChE (Figure 6A, B, C, D). Delta-cadinene, viridiflorol, γ -muurolene and α -caryophyllene were determined to be colocalized with the inhibitor tacrine in the active site of the human BChE

enzyme and the ligand conformations produced by the program was 'true positive' (Figure 7A, B, C, D). In the case of tyrosinase, δ -

cadinene (A) and γ -muurolene (C) are localized around the active site close to the inhibitor (but not fully within the active site), while

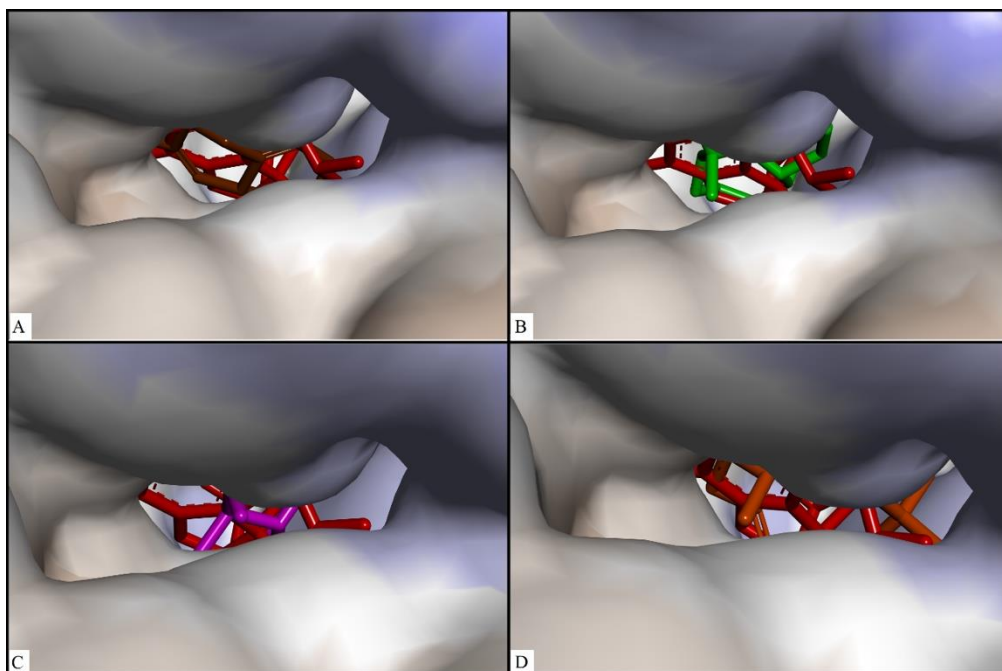


Figure 6. Superposed images of co-crystallized inhibitor (galanthamine, orange) with δ -cadinene (A), viridiflorol (B), γ -muurolene (C), and α -caryophyllene (D) ligands in the active site of human AChE

viridiflorol (B) and α -caryophyllene (D) are localized outside the active site of *B. megaterium* tyrosinase, in a region distant from kojic

acid (red arrows) (Figure 8A, B, C, D). The obtained poses clearly explain the weak binding affinities given for the tyrosinase enzyme

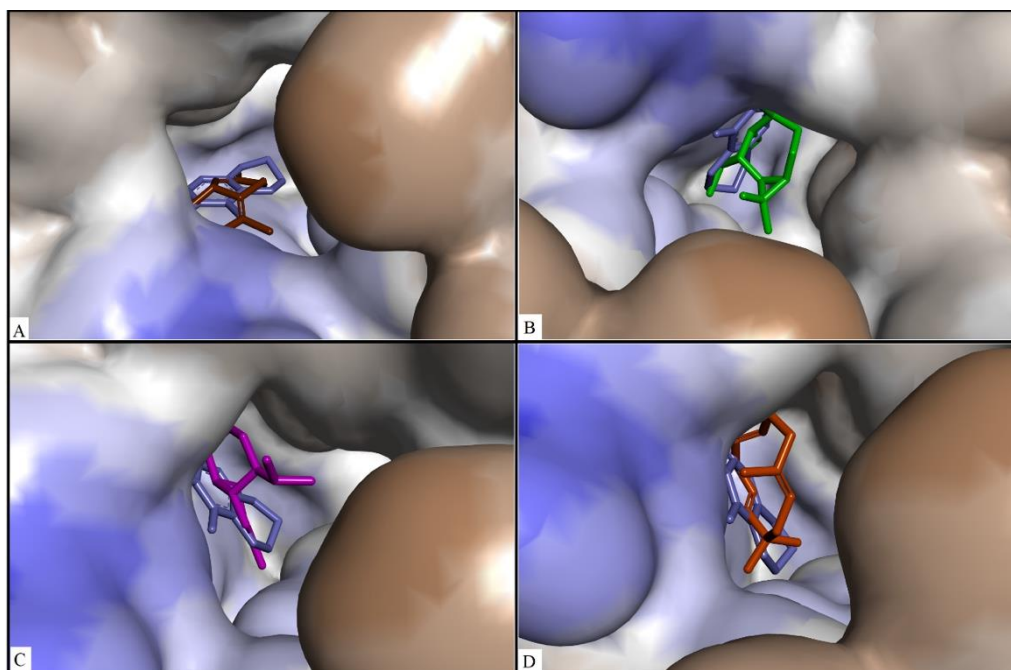


Figure 7. Superposed images of co-crystallized inhibitor (tacrine, grey) with δ -cadinene (A), viridiflorol (B), γ -muurolene (C), and α -caryophyllene (D) ligands in the active site of human BChE

in Table 3. The active site of the tyrosinase is not capable of harboring δ -cadinene, viridiflorol, γ -muurolene and α -caryophyllene due to topological limitations. Therefore, our docking poses verify the experimental results, since it was determined that the tyrosinase inhibitory activity of *S. tomentosa* essential oil was lower

in terms of IC_{50} (1.73 ± 0.03 mg/mL) compared to other enzymes (AChE, BChE and α -amylase). Therefore, it is suggested that a ligand capable of competitively inhibiting the tyrosinase enzyme should not have higher molecular weight and volume values than kojic acid due to the topological restraints in the catalytic region.

In this study, the relative binding capacity index (RBCI), which allows statistical ranking of the activity potentials of phytochemicals by using the binding free energy values obtained from molecular docking calculations, was used (Figure 9 and Table 8) (Istifli et al., 2020). As a result of the RBCI analysis, phytochemicals such as δ -cadinene, viridiflorol, γ -muurolene and α -caryophyllene were determined to be 'hit' components. Top-ranked poses of human

pancreatic α -amylase, human AChE, human BChE and *B. megaterium* tyrosinase enzymes and δ -cadinene, viridiflorol, γ -muurolene and α -caryophyllene are given in Figures 1, 2, 3 and 4, respectively. RBCI analysis also revealed that terpinene-4-ol, camphor and α -pinene were the weakest affinity for these 4 different enzyme targets (Figure 9).

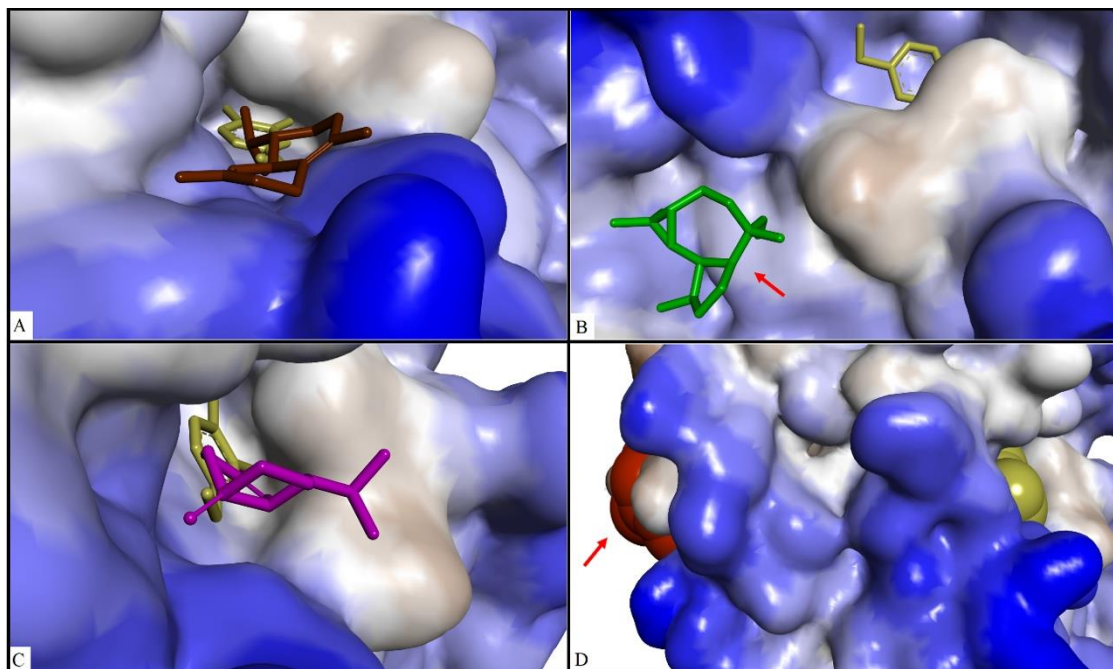


Figure 8. Superposed images of co-crystallized inhibitor (kojic acid, yellow) with δ -cadinene (A), viridiflorol (B), γ -muurolene (C), and α -caryophyllene (D) in the active site of *B. megaterium* tyrosinase

3.6. ADMET and drug-likeness features of hit compounds

In this study, ADMET and drug-likeness properties of δ -cadinene, viridiflorol, γ -muurolene and α -caryophyllene were calculated by entering the SMILES (simplified molecular input line entry specification) characters of 'hit' ligands into the search engines of online pkCSM (<http://biosig.unimelb.edu.au/pkcsml/>) and SwissADME (<http://www.swissadme.ch/>) servers. Considering ADMET properties, none of the 'hit' ligands show AMES toxicity or hepatotoxicity, nor are they a substrate for P-glycoprotein (P-gp). Rat LD₅₀ values range from 1.540 to 1.776 mol/kg and are in an acceptable non-toxic range. On the other hand, blood-brain barrier (BBB) permeability is only detected for the viridiflorol ligand, and all ligands inhibit at least CYP2C19 or CYP2C9 (Table 9). In addition, although viridiflorol exhibits a lower absorption (92.814%) than other ligands in terms of intestinal absorption, it exhibits a higher advantage as a drug candidate due to its low total clearance (0.817 ml/kg). A low total clearance rate indicates that viridiflorol will be excreted more slowly from the body and will therefore require longer dosing intervals in a possible drug administration (Table 9). According to Lipinski's rule of 5, all four 'hit' ligands were showed drug-like properties (Table 10). However, viridiflorol exhibits a more favorable drug-like profile since it does not exceed the MLOGP > 4.15 limit that is violated by the other four ligands. As a result, the 'hit' ligands δ -cadinene, viridiflorol, γ -muurolene and α -caryophyllene, in general, show good pharmacokinetic activity and low toxicity (da Silva Barbosa et al., 2020; Hussein et al., 2019; Schepetkin et al., 2021). Cytochrome P450 (CYP) inhibition, on the other hand, is a common handicap observed in all ligands, and may have adverse effects on the drug metabolism of the host organism.

3.7. Identification of possible intracellular targets of hit compounds

In this study, the most likely intracellular macromolecular targets of hit phytochemicals were documented using the SwissTargetPrediction (<http://www.swisstargetprediction.ch>) web server.

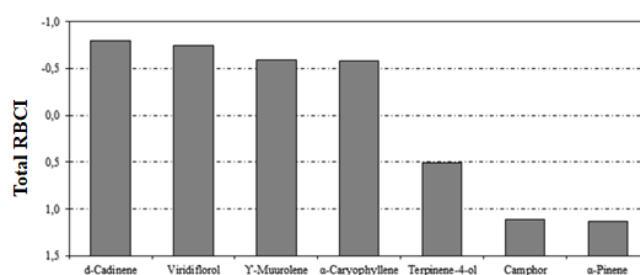


Figure 9. Relative binding capacity index of terpenoids (RBCI)

According to Figure 10A, nuclear receptors (22.9%), various enzymes (20.5%) and family A G protein-coupled receptors (10.8%) constitute the major group of the most likely intracellular targets of δ -cadinene. However, the probability of interaction of δ -cadinene with these proteins was found to be between 0.042 and 0.052 (Table 11), which is not statistically significant. According to Figure 10B, family A G protein-coupled receptors (21%), various enzymes (19%), and extracellular secretory proteins (11%) constitute the most likely intracellular target group of viridiflorol. However, the probability of interaction of viridiflorol with these proteins was found to be between 0.060 and 0.346 (Table 11), which is not

statistically significant. According to Figure 10C, various enzymes (21%), nuclear receptors (21%), and family A G protein-coupled receptors (9%) constitute the most likely intracellular target group of γ -muurolene. However, the probability of interaction of γ -muurolene with these proteins was found to be between 0.042-0.090 (Table 11), which is not statistically significant. According to Figure 10D, family A G protein-coupled receptors (21.4%), nuclear receptors (19%) and various enzymes (19%) constitute the most likely intracellular target group of α -caryophyllene. However, the probability of interaction of α -caryophyllene with these proteins was found to be 0.042 (Table 11), indicating a statistically insignificant outcome.

Table 8. RBCI values of terpenoids

Component	RBCI
δ -cadinene	-0.8
Viridiflorol	-0.7
γ -muurolene	-0.6
α -caryophyllene	-0.6
Terpinene-4-ol	0.5
Camphor	1.1
α -pinene	1.1

4. Conclusions

In this study, the characterization of the chemical composition of *S. tomentosa* essential oil, the α -amylase, α -glucosidase, AChE, BChE and tyrosinase inhibitory activity assays of the dominant compounds, and the possible molecular interactions of the active sites of these enzymes with the major compounds were investigated. Considering the IC_{50} values, it was determined that *S. tomentosa* essential oil showed relatively higher inhibitory activity (IC_{50} = 0.97 mg/mL – 1.35 mg/mL) on the α -glucosidase, BChE and AChE enzymes. On the other hand, α -amylase and tyrosinase inhibitory capacity (IC_{50} = 1.51 mg/mL – 1.73 mg/mL) of *S. tomentosa* essential oil was found to be lower. Molecular docking studies have brought further atomistic perspective to our study in terms of explaining the molecular-scale interactions between the dominant

compounds of *S. tomentosa* essential oil and α -amylase, α -glucosidase, AChE, BChE and tyrosinase as well as the binding mode of ligands. In relative agreement with the experimental inhibition study, the dominant compounds of *S. tomentosa* essential oil (δ -cadinene, viridiflorol, γ -muurolene and α -caryophyllene) displayed high binding affinity (-6.90 – -8.40 kcal/mol) to AChE, BChE and α -amylase and good inhibition constant (K_i = 0.69 μ M – 8.76 μ M). On the other hand, the affinities of these 'hit' compounds to tyrosinase were not found to be energetically highly favorable (-5.50 – -5.90 kcal/mol; K_i = 47 μ M - 93 μ M). Considering their localization around the active site, it was determined that the 'hit' ligands were not suitable for entry into the active site of the tyrosinase enzyme. This finding partially explains why *S. tomentosa* essential oil failed to inhibit the tyrosinase enzyme experimentally. Therefore, docking studies have also revealed that the size of the ligands and the enzyme active sites should be compatible with each other in terms of volume. Considering *in silico* physicochemical properties, drug-likeness (Lipinski's rule of 5) and intracellular targets, δ -cadinene, viridiflorol, γ -muurolene and α -caryophyllene showed 'hit' molecule properties and they did not show non-specific enzyme or protein affinity. However, possible CYP450 inhibitory activities calculated by *in silico* analyzes (especially CYP2C19 and CYP2C9) should also be confirmed experimentally and, if necessary, CYP450 affinities should be reduced by molecular modification so as not to adversely affect the biological activities of the components. In this study, possible AChE, BChE and α -amylase inhibitors and their molecular interaction patterns in the active sites of these targets are proposed. In the light of the results obtained from this study, it was concluded that the dominant interaction pattern of δ -cadinene, viridiflorol, γ -muurolene and α -caryophyllene with AChE, BChE and α -amylase is via hydrophobic contacts and the compatibility between ligand size and active site volume are important factors in enzyme inhibition. Ligand binding tests (LBT) between isolated δ -cadinene, viridiflorol, γ -muurolene and α -caryophyllene and AChE, BChE and α -amylase would constitute the next step in confirming the competitive inhibitory capacity of these proposed 'hit' ligands.

Table 9. Certain ADMET properties of hit terpenoids

Ligand	BBB permeability ^{1,*}	Intestinal absorption (%)	P-gp substrate ^{2,*}	Cytochrome P inhibition ^{3,*}	Total clearance (ml/kg)	AMES Toxicity ⁴	Hepatotoxicity ⁴	Rat LD ₅₀ (mol/kg) ⁴
δ -cadinene	No	96.128	No	Yes (CYP2C19, CYP2C9)	1.182	No	No	1.552
Viridiflorol	Yes	92.814	No	Yes (CYP2C19)	0.817	No	No	1.615
γ -muurolene	No	96.475	No	Yes (CYP2C19, CYP2C9)	1.188	No	No	1.540
α -caryophyllene	No	94.682	No	Yes (CYP2C19)	1.282	No	No	1.766

¹ BBB: Blood-Brain Barrier, ² P-gp: P-glycoprotein substrate, ³ CYP: Cytochrome P, ⁴ <http://biosig.unimelb.edu.au/pkcsmprediction>, ^{*}<https://www.swissadme.ch>

Table 10. Drug-likeness properties of docked hit terpenoids

Ligand	Number of rotatable bonds	TPSA ¹	Consensus Log P	Log S (ESOL ²)	Drug-likeness (Lipinski's rule of 5)
δ -cadinene	1	0.00	4.12	-3.43	Yes; 1 violation (MLOGP>4.15)
Viridiflorol	0	20.23	3.42	-3.57	Yes; 0 violation
γ -muurolene	1	0.00	4.18	-3.76	Yes; 1 violation (MLOGP>4.15)
α -caryophyllene	0	0.00	4.26	-3.97	Yes; 1 violation (MLOGP>4.15)

¹ TPSA: Topological polar surface area (\AA^2), ² ESOL: Estimated water solubility [(Non-soluble < -10 < Poor < -6 < Moderately < -4 < Soluble < -2 < Good < 0 < Highly soluble), according to Delaney, J.S. (2004)]. Data source: <http://www.swissadme.ch/index.php>

Table 11. Probabilities of interaction of hit terpenoids with their putative intracellular targets

Ligand	Probability of interaction with intracellular proteins*	
	Max.	Min.
δ -cadinene	0.052	0.042
Viridiflorol	0.346	0.060
γ -muurolene	0.090	0.042
α -caryophyllene	0.042	0.042

* Values between 0-1 are the probability values that the intracellular protein is the target of the presumed bioactive molecule. A probability value equal to or very close to '1' usually indicates that the molecule under investigation is a known bioactive agent. Source: http://www.swisstargetprediction.ch/help_results.php

Acknowledgments

The data presented here is basically originated from Mr. Mustafa KOCER's M. Sc. thesis. The authors would like to thank to the

Research Council of Kilis 7 Aralik University (project number: 2128LTP1).

Conflict of interest

The author confirms that there are no known conflicts of interest.

CRedit authorship contribution statement

Mustafa Kocer: Conceptualization, Data curation, Investigation, Methodology, Writing, Review & Editing

Erman Salih Istifli: Conceptualization, Data curation, Formal analysis, Investigation, Methodology, Software, Visualization, Writing, Review & Editing

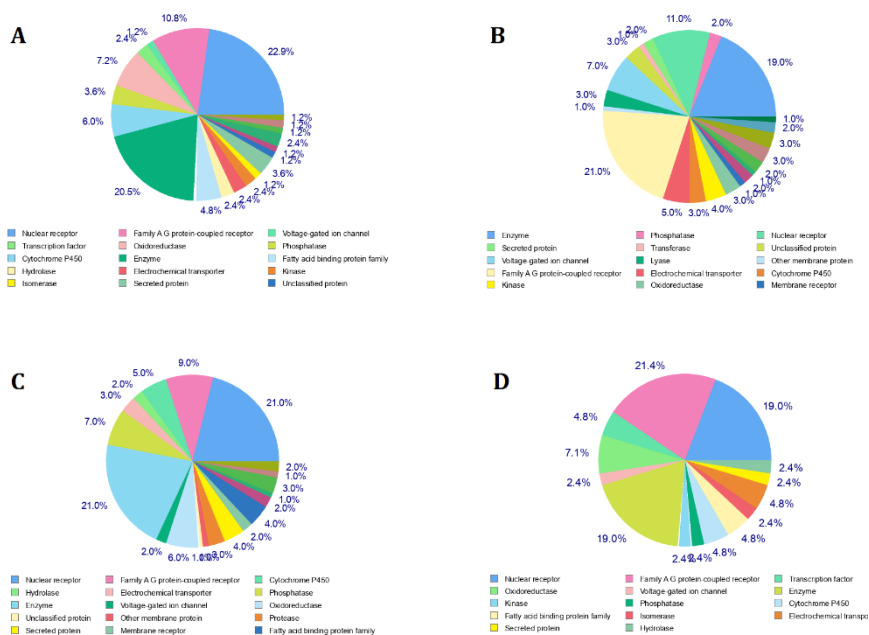


Figure 10. The most likely intracellular macromolecular targets predicted for A - δ -cadinene B - Viridiflorol, C - γ -muurolene and D - α -caryophyllene

ORCID Numbers of the Authors

M. Kocer: 0000-0001-5350-7233

E.S. Istifli: 0000-0003-2189-0703

Supplementary File

None.

References

- Aghajari, N., Feller, G., Gerday, C., Haser, R., 2002. Structural basis of alpha-amylase activation by chloride. *Protein Science*, 11, 1435-1441.
- Ak, G., Zengin, G., Ceylan, R., Fawzi Mahomoodally, M., Jugreet, S., Mollica, A., Stefanucci, A., 2021. Chemical composition and biological activities of essential oils from *Calendula officinalis* L. flowers and leaves. *Flavour and Fragrance Journal*, 36, 554-563.
- Askun, T., Baser, K.H.C., Tumen, G., Kurkcuoglu, M., 2010. Characterization of essential oils of some *Salvia* species and their antimycobacterial activities. *Turkish Journal of Biology*, 34, 89-95.
- Ballante, F., 2018. Protein-Ligand Docking in Drug Design: Performance Assessment and Binding-Pose Selection. *Methods in Molecular Biology*, 1824, 67-88.

- Bardackci, H., Servi, H., Polatoglu, K., 2019. Essential Oil Composition of *Salvia candidissima* Vahl. *occidentalis* Hedge, *S. tomentosa* Miller and *S. heldreichiana* Boiss. Ex Benth from Turkey. *Journal of Essential Oil Bearing Plants*, 22, 1467-1480.
- Bonesi, M., Menichini, F., Tundis, R., Loizzo, M.R., Conforti, F., Passalacqua, N.G., Statti, G.A., Menichini, F., 2010. Acetylcholinesterase and butyrylcholinesterase inhibitory activity of *Pinus* species essential oils and their constituents. *Journal of Enzyme Inhibition and Medicinal Chemistry*, 25, 622-628.
- Bouyahya, A., Lagrouh, F., El Omari, N., Bourais, I., El Jemli, M., Marmouzi, I., Salhi, N., Faouzi, M.E., Belmehti, O., Dakka, N., Bakri, Y., 2020. Essential oils of *Mentha viridis* rich phenolic compounds show important antioxidant, antidiabetic, dermatoprotective, antidermatophyte and antibacterial properties. *Biocatalysis and Agricultural Biotechnology*, 23, 101471.
- Brayer, G.D., Luo, Y., Withers, S.G., 1995. The structure of human pancreatic α -amylase at 1.8 Å resolution and comparisons with related enzymes. *Protein Science*, 4, 1730-1742.
- Burlando, B., Clericuzio, M., Cornara, L., 2017. Moraceae plants with tyrosinase inhibitory activity: A review. *Mini Reviews in Medicinal Chemistry*, 17, 108-121.
- Chang, T.S., 2009. An updated review of tyrosinase inhibitors. *International Journal of Molecular Sciences*, 10, 2440-2475.
- Chang, T.S., 2012. Natural melanogenesis inhibitors acting through the down-regulation of tyrosinase activity. *Materials*, 5, 1661-1685.
- Chaudhury, A., Duvoor, C., Reddy Dendi, V.S., Kraleti, S., Chada, A., Ravilla, R., Marco, A., Shekhawat, N.S., Montales, M.T., Kuriakose, K., 2017. Clinical review of antidiabetic drugs: implications for type 2 diabetes mellitus management. *Frontiers in Endocrinology*, 8, 6.
- da Silva Barbosa, D.C., Holanda, V.N., de Assis, C.R.D., de Oliveira Farias, J.C.R., Henrique da Nascimento, P., da Silva, W.V., Navarro, D.M.D.A.F., da Silva, M.V., de Menezes

- Lima, V.L., dos Santos Correia, M.T., 2020. Chemical composition and acetylcholinesterase inhibitory potential, in silico, of *Myrciaria floribunda* (H. West ex Willd.) O. Berg fruit peel essential oil. *Industrial Crops and Products*, 151, 112372.
- Daina, A., Michielin, O., Zoete, V., 2017. SwissADME: a free web tool to evaluate pharmacokinetics, drug-likeness and medicinal chemistry friendliness of small molecules. *Scientific Reports*, 7, 1-13.
- Daina, A., Michielin, O., Zoete, V., 2019. SwissTargetPrediction: updated data and new features for efficient prediction of protein targets of small molecules. *Nucleic Acids Research*, 47, W357-W364.
- Davis, E.C., Callender, V.D., 2010. Postinflammatory hyperpigmentation: a review of the epidemiology, clinical features, and treatment options in skin of color. *The Journal of Clinical and Aesthetic Dermatology*, 3, 20.
- Delaney, J.S., 2004. ESOL: estimating aqueous solubility directly from molecular structure. *Journal of Chemical Information and Modeling*, 44, 1000-1005.
- Dos Santos, R.N., Ferreira, L.G., Andricopulo, A.D., 2018. Practices in Molecular Docking and Structure-Based Virtual Screening. *Methods in Molecular Biology*, 1762, 31-50.
- Edwin, E., Sheeja, E., Chaturvedi, M., Sharma, S., Gupta, V., 2006. A comparative study on antihyperglycemic activity of fruits and barks of *Ficus bengalensis* (L.). *Advances in Pharmacology and Toxicology*, 7, 69-71.
- Elgamal, A.M., Ahmed, R.F., Abd-ElGawad, A.M., El Gendy, A.G., Elshamy, A.I., Nassar, M.I., 2021. Chemical Profiles, Anticancer, and Anti-Aging Activities of Essential Oils of *Pluchea dioscoridis* (L.) DC. and *Erigeron bonariensis* L. *Plants-Basel*, 10, 667.
- Elman, G.L., Courtney, K.D., Andres Jr, V., Featherstone, R.M., 1961. A new and rapid colorimetric determination of acetylcholinesterase activity. *Biochemical Pharmacology*, 7, 88-95.
- Erdogan-Orhan, I., Baki, E., Senol, S., Yilmaz, G., 2010. Sage-called plant species sold in Turkey and their antioxidant activities. *Journal of the Serbian Chemical Society*, 75, 1491-1501.
- Ertas, A., Goren, A.C., Boga, M., Yesil, Y., Kolak, U., 2014. Essential oil compositions and anticholinesterase activities of two edible plants *Tragopogon latifolius* var. *angustifolius* and *Lycopsis orientalis*. *Natural Product Research*, 28, 1405-1408.
- Es-Safi, I., Mechchate, H., Amaghnoouj, A., El Moussaoui, A., Cerruti, P., Avella, M., Grafov, A., Bousta, D., 2021. Marketing and legal status of phytomedicines and food supplements in Morocco. *Journal of Complementary and Integrative Medicine*, 18, 279-285.
- Ferrante, C., Zengin, G., Menghini, L., Diuzheva, A., Jeko, J., Cziaki, Z., Recinella, L., Chivaroli, A., Leone, S., Brunetti, L., Lobine, D., Senkardes, I., Mahomoodally, M.F., Orlando, G., 2019. Qualitative Fingerprint Analysis and Multidirectional Assessment of Different Crude Extracts and Essential Oil from Wild *Artemisia santonicum* L. *Processes*, 7, 522.
- Ferreira, L.G., Dos Santos, R.N., Oliva, G., Andricopulo, A.D., 2015. Molecular docking and structure-based drug design strategies. *Molecules*, 20, 13384-13421.
- Fukai, T., Oku, Y., Hou, A.J., Yonekawa, M., Terada, S., 2005. Antimicrobial activity of isoprenoid-substituted xanthenes from *Cudrania cochinchinensis* against vancomycin-resistant enterococci. *Phytomedicine*, 12, 510-513.
- Hanlidou, E., Karousou, R., Lazari, D., 2014. Essential-Oil Diversity of *Salvia tomentosa* Mill. in Greece. *Chemistry & Biodiversity*, 11, 1205-1215.
- Hanwell, M.D., Curtis, D.E., Lonie, D.C., Vandermeersch, T., Zurek, E., Hutchison, G.R., 2012. Avogadro: an advanced semantic chemical editor, visualization, and analysis platform. *Journal of Cheminformatics*, 4, 1-17.
- Haznedaroglu, M.Z., Karabay, N.U., Zeybek, U., 2001. Antibacterial activity of *Salvia tomentosa* essential oil. *Fitoterapia*, 72, 829-831.
- Ho, J.C., 2010. Chemical Composition and Bioactivity of Essential Oil of Seed and Leaf from *Alpinia speciosa* Grown in Taiwan. *Journal of the Chinese Chemical Society*, 57, 758-763.
- Huang, S.Y., Zou, X., 2010. Advances and challenges in protein-ligand docking. *International Journal of Molecular Sciences*, 11, 3016-3034.
- Hussein, B.A., Karimi, I., Yousofvand, N., 2019. Computational insight to putative anti-acetylcholinesterase activity of *Commiphora myrrha* (Nees), Engler, Burseraceae: a lesson of archaeopharmacology from Mesopotamian Medicine I. *In Silico Pharmacology*, 7, 1-17.
- Istifli, E.S., Tepe, A.Ş., Sarikürkcü, C., Tepe, B., 2020. Interaction of certain monoterpenoid hydrocarbons with the receptor binding domain of 2019 novel coronavirus (2019-nCoV), transmembrane serine protease 2 (TMPRSS2), cathepsin B, and cathepsin L (CatB/L) and their pharmacokinetic properties. *Turkish Journal of Biology*, 44, 242-264.
- Jugreet, B.S., Mahomoodally, M.F., Sinan, K.I., Zengin, G., Abdallah, H.H., 2020. Chemical variability, pharmacological potential, multivariate and molecular docking analyses of essential oils obtained from four medicinal plants. *Industrial Crops and Products*, 150, 112394.
- Karimi, I., Yousofvand, N., Hussein, B.A., 2021. *In vitro* cholinesterase inhibitory action of *Cannabis sativa* L. Cannabaceae and *in silico* study of its selected phytocompounds. *In Silico Pharmacology*, 9, 1-15.
- Ko, H.H., Chiang, Y.C., Tsai, M.H., Liang, C.J., Hsu, L.F., Li, S.Y., Wang, M.C., Yen, F.L., Lee, C.W., 2014. Eupafolin, a skin whitening flavonoid isolated from *Phylla nodiflora*, downregulated melanogenesis: Role of MAPK and Akt pathways. *Journal of Ethnopharmacology*, 151, 386-393.
- Li, B., Duysen, E.G., Carlson, M., Lockridge, O., 2008. The butyrylcholinesterase knockout mouse as a model for human butyrylcholinesterase deficiency. *Journal of Pharmacology and Experimental Therapeutics*, 324, 1146-1154.
- Lien, C.Y., Chen, C.Y., Lai, S.T., Chan, C.F., 2014. Kinetics of mushroom tyrosinase and melanogenesis inhibition by N-acetyl-pentapeptides. *The Scientific World Journal*, 2014.
- Lohning, A.E., Levison, S.M., Williams-Noonan, B., Schweiker, S.S., 2017. A Practical Guide to Molecular Docking and Homology Modelling for Medicinal Chemists. *Current Topics in Medicinal Chemistry*, 17, 2023-2040.
- Lopez-Vallejo, F., Caulfield, T., Martinez-Mayorga, K., Giulianotti, M.A., Nefzi, A., Houghton, R.A., Medina-Franco, J.L., 2011. Integrating virtual screening and combinatorial chemistry for accelerated drug discovery. *Combinatorial Chemistry & High Throughput Screening*, 14, 475-487.
- Lopez, M.D., Campoy, F.J., Pascual-Villalobos, M.J., Munoz-Delgado, E., Vidal, C.J., 2015. Acetylcholinesterase activity of electric eel is increased or decreased by selected monoterpenoids and phenylpropanoids in a concentration-dependent manner. *Chemico-Biological Interactions*, 229, 36-43.
- Majouli, K., Hlila, M.B., Hamdi, A., Flamini, G., Ben Jannet, H., Kenani, A., 2016. Antioxidant activity and alpha-glucosidase inhibition by essential oils from *Hertia cheirifolia* (L.). *Industrial Crops and Products*, 82, 23-28.
- Mechchate, H., Es-safi, I., Bari, A., Grafov, A., Bousta, D., 2020. Ethnobotanical survey about the management of diabetes with medicinal plants used by diabetic patients in region of Fez-Meknes, Morocco. *Journal of Ethnobotany Research and Applications*, 19, 1-28.
- Mechchate, H., Es-Safi, I., Haddad, H., Bekkari, H., Grafov, A., Bousta, D., 2021a. Combination of Catechin, Epicatechin, and Rutin: optimization of a novel complete antidiabetic formulation using a mixture design approach. *The Journal of Nutritional Biochemistry*, 88, 108520.
- Mechchate, H., Es-Safi, I., Louba, A., Alqahtani, A.S., Nasr, F.A., Noman, O.M., Farooq, M., Alharbi, M.S., Alqahtani, A., Bari, A., 2021b. *In vitro* alpha-amylase and alpha-glucosidase inhibitory activity and *in vivo* antidiabetic activity of *Withania frutescens* L. Foliar extract. *Molecules*, 26, 293.
- Meng, X.-Y., Zhang, H.-X., Mezei, M., Cui, M., 2011. Molecular docking: a powerful approach for structure-based drug discovery. *Current Computer-Aided Drug Design*, 7, 146-157.
- Murata, K., Takahashi, K., Nakamura, H., Itoh, K., Matsuda, H., 2014. Search for skin-whitening agent from *Prunus* plants and the molecular targets in melanogenesis pathway of active compounds. *Natural Product Communications*, 9, 185-188.
- Nagy, G., Günther, G., Máthé, I., Blunden, G., Yang, M.-h., Crabb, T.A., 1999. Diterpenoids from *Salvia glutinosa*, *S. austriaca*, *S. tomentosa* and *S. verticillata* roots. *Phytochemistry*, 52, 1105-1109.
- Noh, H., Lee, S.J., Jo, H.-J., Choi, H.W., Hong, S., Kong, K.-H., 2020. Histidine residues at the copper-binding site in human tyrosinase are essential for its catalytic activities. *Journal of Enzyme Inhibition and Medicinal Chemistry*, 35, 726-732.
- Orhan, D.D., Senol, F.S., Hosbas, S., Orhan, I.E., 2014. Assessment of cholinesterase and tyrosinase inhibitory and antioxidant properties of *Viscum album* L. samples collected from different host plants and its two principal substances. *Industrial Crops and Products*, 62, 341-349.
- Orhan, I.E., Jedrejek, D., Senol, F.S., Salmas, R.E., Durdagi, S., Kowalska, I., Pecio, L., Oleszek, W., 2018. Molecular modeling and *in vitro* approaches towards cholinesterase inhibitory effect of some natural xanthohumol, naringenin, and acyl phloroglucinol derivatives. *Phytomedicine*, 42, 25-33.
- Orhan, I.E., Kucukboyaci, N., Calis, I., Cerón-Carrasco, J.P., den-Haan, H., Peña-García, J., Pérez-Sánchez, H., 2017. Acetylcholinesterase inhibitory assessment of isolated constituents from *Salsola grandis* Freitag, Vural & Adigüzel and molecular modeling studies on N-acetyltryptophan. *Phytochemistry Letters*, 20, 373-378.
- Özcan, M., Akgül, A., Chalchat, J., 2002. Volatile constituents of essential oils of *Salvia aucheri* Benth. var. *canescens* Boiss. et Heldr. and *S. tomentosa* Mill. grown in Turkey. *Journal of Essential Oil Research*, 14, 339-341.
- Palanisamy, U.D., Ling, L.T., Manaharan, T., Appleton, D., 2011. Rapid isolation of geraniin from *Nephelium lappaceum* rind waste and its anti-hyperglycemic activity. *Food Chemistry*, 127, 21-27.
- Pérez Gutierrez, R., Hernández Luna, H., Hernández Garrido, S., 2006. Antioxidant activity of *Tagetes erecta* essential oil. *Journal of the Chilean Chemical Society*, 51, 883-886.
- Perry, E., Howes, M.J.R., 2011. Medicinal plants and dementia therapy: herbal hopes for brain aging? *CNS Neuroscience & Therapeutics*, 17, 683-698.
- Perry, N.S.L., Houghton, P.J., Theobald, A., Jenner, P., Perry, E.K., 2000. *In-vitro* inhibition of human erythrocyte acetylcholinesterase by *Salvia lavandulaefolia* essential oil and constituent terpenes. *Journal of Pharmacy and Pharmacology*, 52, 895-902.
- Pettersen, E.F., Goddard, T.D., Huang, C.C., Couch, G.S., Greenblatt, D.M., Meng, E.C., Ferrin, T.E., 2004. UCSF Chimera--a visualization system for exploratory research and analysis. *Journal of Computational Chemistry*, 25, 1605-1612.
- Pinho, B.R., Ferreres, F., Valentão, P., Andrade, P.B., 2013. Nature as a source of metabolites with cholinesterase-inhibitory activity: an approach to Alzheimer's disease treatment. *Journal of Pharmacy and Pharmacology*, 65, 1681-1700.
- Pires, D.E., Blundell, T.L., Ascher, D.B., 2015. pkCSM: Predicting Small-Molecule Pharmacokinetic and Toxicity Properties Using Graph-Based Signatures. *Journal of Medicinal Chemistry*, 58, 4066-4072.
- Politeo, O., Bektašević, M., Carev, I., Jurin, M., Roje, M., 2018. Phytochemical composition, antioxidant potential and cholinesterase inhibition potential of extracts from *Mentha pulegium* L. *Chemistry & Biodiversity*, 15, e1800374.
- Rosenberry, T.L., Brazzolotto, X., Macdonald, I.R., Wandhammer, M., Trovaslet-Leroy, M., Darvesh, S., Nachon, F., 2017. Comparison of the Binding of Reversible Inhibitors to Human Butyrylcholinesterase and Acetylcholinesterase: A Crystallographic, Kinetic and Calorimetric Study. *Molecules*, 22, 2098.
- Sacks, D.B., 1997. Implications of the revised criteria for diagnosis and classification of diabetes mellitus. Oxford University Press.

- Salleh, W., Ahmad, F., Yen, K.H., 2015. Chemical compositions and biological activities of the essential oils of *Beilschmiedia madang* Blume (Lauraceae). *Archives of Pharmacol Research*, 38, 485-493.
- Sarikurkcu, C., Zengin, G., Oskay, M., Uysal, S., Ceylan, R., Aktumsek, A., 2015. Composition, antioxidant, antimicrobial and enzyme inhibition activities of two *Origanum vulgare* subspecies (subsp. *vulgare* and subsp. *hirtum*) essential oils. *Industrial Crops and Products*, 70, 178-184.
- Savelev, S., Okello, E., Perry, N.S.L., Wilkins, R.M., Perry, E.K., 2003. Synergistic and antagonistic interactions of anticholinesterase terpenoids in *Salvia lavandulaefolia* essential oil. *Pharmacology Biochemistry and Behavior*, 75, 661-668.
- Chepetkin, I.A., Özek, G., Özek, T., Kirpotina, L.N., Khlebnikov, A.I., Quinn, M.T., 2021. Chemical Composition and Immunomodulatory Activity of Essential Oils from *Rhododendron albiflorum*. *Molecules*, 26, 3652.
- Sinan, K.I., Etienne, O.K., Stefanucci, A., Mollica, A., Mahomoodally, M.F., Jugreet, S., Rocchetti, G., Lucini, L., Aktumsek, A., Montesano, D., 2021. Chemodiversity and biological activity of essential oils from three species from the *Euphorbia* genus. *Flavour and Fragrance Journal*, 36, 148-158.
- Solano, F., 2018. On the Metal Cofactor in the Tyrosinase Family. *International Journal of Molecular Sciences*, 19, 633.
- Soltanbeigi, A., Sakartepe, E., 2020. Chemical specification of Wild *Salvia tomentosa* Mill. collected From Inner Aegean Region of Turkey. *Zeitschrift für Arznei- & Gewerzpflanzen*, 25, 31-35.
- Tepe, B., Daferera, D., Sokmen, A., Sokmen, M., Polissiou, M., 2005. Antimicrobial and antioxidant activities of the essential oil and various extracts of *Salvia tomentosa* Miller (Lamiaceae). *Food Chemistry*, 90, 333-340.
- Trott, O., Olson, A.J., 2010. AutoDock Vina: improving the speed and accuracy of docking with a new scoring function, efficient optimization, and multithreading. *Journal of Computational Chemistry*, 31, 455-461.
- Tsai, C.-C., Chan, C.-F., Huang, W.-Y., Lin, J.-S., Chan, P., Liu, H.-Y., Lin, Y.-S., 2013. Applications of *Lactobacillus rhamnosus* spent culture supernatant in cosmetic antioxidation, whitening and moisture retention applications. *Molecules*, 18, 14161-14171.
- Ulubelen, A., Miski, M., Mabry, T., 1981a. Further flavones and triterpenes and the new 6-hydroxyluteolin 5- β -D-glucoside from *Salvia tomentosa*. *Journal of Natural Products*, 44, 586-587.
- Ulubelen, A., Miski, M., Mabry, T., 1981b. A new diterpene acid from *Salvia tomentosa*. *Journal of Natural Products*, 44, 119-124.
- Ulukanli, Z., Karaborklu, S., Cenet, M., Sagdic, O., Ozturk, I., Balcilar, M., 2013. Essential oil composition, insecticidal and antibacterial activities of *Salvia tomentosa* Miller. *Medicinal Chemistry Research*, 22, 832-840.
- Usman, L.A., Oguntoyey, O.S., Ismaeel, R.O., 2020. Effect of Seasonal Variation on Chemical Composition, Antidiabetic and Antioxidant Potentials of Leaf Essential Oil of *Eucalyptus globulus* L. *Journal of Essential Oil Bearing Plants*, 23, 1314-1323.
- Valdes-Tresanco, M.S., Valdes-Tresanco, M.E., Valiente, P.A., Moreno, E., 2020. AMDock: a versatile graphical tool for assisting molecular docking with Autodock Vina and Autodock4. *Biology Direct*, 15, 1-12.
- Wang, Z., Sun, H., Shen, C., Hu, X., Gao, J., Li, D., Cao, D., Hou, T., 2020. Combined strategies in structure-based virtual screening. *Physical Chemistry Chemical Physics*, 22, 3149-3159.
- Wild, S., Roglic, G., Green, A., Sicree, R., King, H., 2004. Global prevalence of diabetes: estimates for the year 2000 and projections for 2030. *Diabetes Care*, 27, 1047-1053.
- Yang, C.H., Huang, Y.C., Tsai, M.L., Cheng, C.Y., Liu, L.L., Yen, Y.W., Chen, W.L., 2015. Inhibition of melanogenesis by beta-caryophyllene from lime mint essential oil in mouse B16 melanoma cells. *International Journal of Cosmetic Science*, 37, 550-554.
- Yang, Y., Meng, J., Liu, C., Zhang, Y., Tian, J., Gu, D., 2019. GC-MS profiling, bioactivities and *in silico* theoretical explanation of cone oil from *Pinus thunbergii* Parl. *Industrial Crops and Products*, 141, 111765.
- Yilar, M., Kadioglu, I., Telci, I., 2018. Chemical composition and antifungal activity of *Salvia officinalis* (L.), *S. Cryptantha* (Montbret et aucher ex Benth.), *S. tomentosa* (MILL.) plant essential oils and extracts. *Fresenius Environmental Bulletin*, 27, 1695-1706.
- Zengin, G., Sarikurkcu, C., Aktumsek, A., Ceylan, R., 2014. *Sideritis galatica* Bornm.: A source of multifunctional agents for the management of oxidative damage, Alzheimer's and diabetes mellitus. *Journal of Functional Foods*, 11, 538-547.

Reviewed by:

Yavuz Selim CAKMAK: Aksaray University, Aksaray, TURKEY
Muhsin KONUK: Uskudar University, Istanbul, TURKEY

Publisher's Note: All claims expressed in this article are solely those of the authors and do not necessarily represent those of their affiliated organizations, or those of the publisher, the editors and the reviewers. Any product that may be evaluated in this article, or claim that may be made by its manufacturer, is not guaranteed or endorsed by the publisher.



This is an open-access article distributed under the terms of the Creative Commons Attribution 4.0 International License (CC BY). The use, distribution or reproduction in other forums is permitted, provided the original author(s) and the copyright owner(s) are credited and that the original publication in this journal is cited, in accordance with accepted academic practice. No use, distribution or reproduction is permitted which does not comply with these terms.